

# 3rd Korea-Japan Joint International Workshop : Present Earth Surface Processes and Historical Environmental Changes in East Asia

year	2006-01-01
URL	<a href="http://hdl.handle.net/2297/3418">http://hdl.handle.net/2297/3418</a>

□ Title of the Symposium:

3<sup>rd</sup> Japan-Korea Joint International Workshop “Present earth surface processes and historical environmental changes in East Asia”

□ Organizer:

Organized by

Korea Institute of Geoscience and Mineral Resources (KIGAM)

In collaboration with:

Institute of Nature and Environmental Technology, Kanazawa University  
Kanazawa University 21st-century COE Program

Supported by

The Korean Quaternary Association, Korea

Kangwon National University, Korea

Chonnam National University, Korea

Kyunghee University, Korea

Nagoya University, Japan

□ Participants from:

Japan, China and Korea

□ Date: September 26 - 30, 2006

□ Venue: The Korean Federation of Science and Technology Societies (KOFST)

□ Purpose and Scope of the Symposium

The purpose of the Joint workshop is to exchange modern and historical environmental information in Korea and Japan for clarifying environmental processes and changes since the last interglacial in East Asia. Terrestrial sediment records including lacustrine sediment records, have some advantages compared with other proxy data: they include high-resolution records for catchment environment, not only natural records but also artificial ones. With the appropriate approach and methods, the environmental information from terrestrial records and catchment records can provide the clues of detailed environmental processes and changes in climatically, tectonically and anthropogenically sensitive regions such as East Asia. East Asia around Korea and Japan includes industrially developed and developing areas and has experienced various stages of modern industrialization, giving profound influence on environmental changes in the areas. This means that precious information on artificial environment as well as natural one is available for future prediction here.

In this workshop, we will mainly discuss two time domain; present environmental processes (0-100 years) and ancient environmental changes (older than 2000 years) in some lake-catchment systems of western central Korea and central Japan. Both of these areas have many historical records, which may be proxies for natural environmental information as well as artificial one. Lacustrine sediment information here may also include some records on anthropological environment in addition to climatic and hydrogeomorphic environment.

Some lake-catchment systems in both areas have been observed with instruments including sediment traps for these years. Observation for the lake-catchment systems is of great use for understanding environmental processes and mechanism. These indicate that observation-based and process-based information in recent periods can be compared to long-term information in a lake-catchment system. The past is a key to the future, through the present. Paleo-information can be suitably used for considering the future in these fields.

In the workshop, most issues to be studied in each field will be reported and discussed. Among them some issues to be discussed more thoroughly will be chosen as topics for next Symposium in Japan. The issues will be studied further and more information on them will be collected till then.

□ Symposium Program

<b>2006. 09. 27. (wed.)</b>	
<b>09:00</b>	<b>Registration</b>
:20	
:40	
<b>10:00</b>	<b>Opening Address / Congratulatory Speech</b>
:20	<b>Group Photo / Coffee Break</b>
:40	<b>A. Orkhonselenge <i>et al.</i></b> : Soil erosion assessment using radionuclide <sup>137</sup> Cs in South Korea
<b>11:00</b>	<b>J.K. Kim <i>et al.</i></b> : The expansion of gully in the mountainous slope, South Korea
:20	<b>Y. Tanaka <i>et al.</i></b> : Difference in Surface erosion in granite, gneiss and sedimentary rock catchments
:40	<i>Coffee Break</i>
<b>12:00</b>	<b>Y. Onda <i>et al.</i></b> : Investigating infiltration rate, erosion rates and erosion processes within a Japanese cypress plantation using Cs-137 and Pb-210ex measurements
:20	<b>K. Fukushi <i>et al.</i></b> : Behavior of As in low crystalline iron oxide during the alteration process in acid mine drainage environments
:40	<b>Lunch</b>
<b>14:00</b>	<b>S. Yi <i>et al.</i></b> : Palynofloras evidence for historical state of the Golden Crown Gaya (3-7th centuries AD) in the Gimhae fluvial plain, Southern Korean Peninsula
:20	<b>X. Yang</b> : Limnological response to climate changes over the past 200 yr in Namu Co, Central Tibet
:40	<b>E. Ryu <i>et al.</i></b> : Diatom record of the Late Quaternary in the East/Japan Sea
<b>15:00</b>	<i>Coffee Break</i>

- :20** **Y. Wu *et al.*** : Nutrient sources and paleoproductivity during the past century in Longgan Lake, middle reaches of Yangtze River, China
- :40** **Y. Aota *et al.*** : Seasonal change of particulate matter transport and vertical water mixing processes with climatic changes in Lake Biwa
- 16:00** **W.H. Nahm *et al.*** : Environmental records for recent decades in Jinheung Pond sediments (Jeongeup, Jeollabukdo, Korea)
- :20**
- :40** **A. Sakaguchi *et al.*** : U and Th Isotopes in lake sediments, Lake Biwa system in Japan: to obtain insight to their paleoenvironmental implications
- 17:00** **M. Yamamoto *et al.*** : Uranium-series disequilibrium application to lake sediments in geochronology- a short general review
- :20** **T.B. Kim *et al.*** : Development of 2D FEM algorithm for bed elevation change in a curved channel

*Coffee Break*

*Banquet*

**2006. 09. 28. (thu.)**

- 09:00** **K. Kashiwaya** : Lake-catchment system and kosa-covering area in East Eurasia
- :20** **Y. Chun** : Historical records of Asian dust events (Hwangsa) in Korea
- :40** **J. Kim & J. Lee** : Detection of Yellow Sand Dust from multiplex satellite measurements
- 10:00**
- :20** **S.J. Kim & B.Y. Lee** : Simulation of East Asia climate change for the Last Glacial Maximum
- :40** **K.S. Woo & K.N. Jo** : Five years of monsoonal record in the Soda Straw of Seopdong Cave, Korea
- 11:00** **J.C. Kim *et al.*** : The origin of erratic calcite speleothems in the Dangcheomul Lava Tube, Jeju Island, Korea
- :20**
- :40** **J.Y. Kim *et al.*** : Paleosols sequence of Last Glacial Maximum of S. Korea
- 12:00** **A.F. Jin** : A climate change in the Tumen River Basin
- :20** **C.J. Li** : The natural surroundings of Yanbian area

*Coffee Break*

*Coffee Break*

*Lunch*

*Poster Session*

**2006. 09. 29. (fri.)**

*Field Excursion*

Tidal flat sites at Ganghwhado

*Lunch*

- Cultural Sites at Ganghwhado

*Farewell Party*

□ Abstracts of the presented papers

[O-1]

## Soil erosion assessment using radionuclide $^{137}\text{Cs}$ in South Korea

ORKHONSELENGE ALEXANDER<sup>1</sup>, YUKIYA TANAKA<sup>1</sup>, Y. K. KIM<sup>2</sup>

<sup>1</sup>*Department of Geography, Kyunghee University, Seoul 130-701, Korea (alorsel@khu.ac.kr)*

<sup>2</sup>*Korean Atomic Energy Research Institute, Daejeon, Korea*

### Introduction

Radionuclide  $^{137}\text{Cs}$ , which was strongly absorbed into fine particles on ground surfaces worldwide due to testing of thermonuclear weapons from the early 1950s, has been used as a universal tracer to estimate the rates of soil erosion and sedimentation during last two decades. The investigation has also contributed to the development of geomorphologic research methods, particularly, assessment of soil erosion on upper slopes, sediment redeposition on down slopes and associated the rate of soil loss within the catchments using spatially distributed diffusions of radionuclide  $^{137}\text{Cs}$  inventory. In order to estimate the soil erosion in South Korea, spatial variability of radionuclide  $^{137}\text{Cs}$  was measured in three different bedrock catchments underlain by granite (Gr), gneiss (Gn) and sedimentary (Se) rocks. The main cause of the soil erosion here becomes water rather than to wind due to rainfall amount and intensity. The underlying purpose of the present study was to develop an understanding on the medium, short-term intensity and rates of soil erosion using spatial distribution of the radionuclide  $^{137}\text{Cs}$  in these catchments. Thus, the soil erosion and sediment deposition rates were determined by comparing  $^{137}\text{Cs}$  inventories within the catchments with  $^{137}\text{Cs}$  inventories in uneroded soils at these representative reference sites in each catchment area.

### Methods

In order to estimate the spatial distribution of  $^{137}\text{Cs}$  inventory, soil samplings were measured using bulk and core sampling methods between March, 2004 and March, 2005. Bulk samples were collected within the top 10 cm depth from different landform points along the hillslopes as random samplings depending on several main factors, such as landform, slope and elevation within the catchments. Using a soil core sampler, core samples were collected within the top 30 cm depth from different landforms such as head slopes (backslopes), crest flats (summit slopes), crest slopes (shoulder slopes) and head hollows (toeslopes and footslopes). The quantitative  $^{137}\text{Cs}$  inventories

and soil physical properties at incremental samples were determined at intervals of 2cm depth. 42 soil core samples and 44 soil bulk samples were taken from each of the different catchments, making a total of 625 soil samples.  $^{137}\text{Cs}$  radionuclide in the soil samples were analyzed using Gamma-Ray Spectrometry, HPGe detector, Ortec 919E (Model GMK50F), counting the gamma emission for 7200 seconds and estimating the photo peak at 662 keV at the KAERI (Korean Atomic Energy Research Institute). The  $^{137}\text{Cs}$  activity was expressed on a mass basis as becquerels.

## Results

The spatial distribution of the  $^{137}\text{Cs}$  within the soil profiles was related to soil properties rather than to rainfall amount. The  $^{137}\text{Cs}$  inventory was widely distributed in soils containing high organic matter content and clay content. Other geomorphic factors such as surface altitude, slope angle and soil permeability poorly influenced on the spatial distribution of the  $^{137}\text{Cs}$  inventory within soils. The spatial distribution of the radionuclide  $^{137}\text{Cs}$  indicated that the average areal activities of the baseline  $^{137}\text{Cs}$  inventories in uneroded soils were 2100 Bq/m<sup>2</sup> in the Gr catchment, 2840 Bq/m<sup>2</sup> in the Gn catchment and 3366 Bq/m<sup>2</sup> in the Se catchment (Table 1). At most sampling points, the vertical variability of the  $^{137}\text{Cs}$  inventory in the profiles showed an exponential curve with soil depths, having the highest inventories in the surface layers that gradually decrease along the soil profiles of these catchments. The intensity of the soil erosion within the catchments was estimated based on the loss of the  $^{137}\text{Cs}$  inventory in lateral and vertical distributions. The spatial distributions of the  $^{137}\text{Cs}$  inventory within the catchments indicate that soils are lost positively by losses of the  $^{137}\text{Cs}$  inventory in soil. The soil erosion in these catchments underlain by different bedrocks showed the general geomorphologic features having no distinctive differences to each other for landscape changes. In particular, the straight parts of middle slopes and upper slopes are more sensitive to erosion processes compared to crest flats and lower slopes in these catchments. However, the rates of soil erosion in the granite catchment indicated the significant higher rate than in the gneiss and sedimentary catchments. In particular, the average erosion rates were calculated as 40.71 t/ha/yr, 26.56 t/ha/yr and 22.27 t/ha/yr in the Gr, Gn and Se catchments, respectively. These rates indicate that erosion processes on hillslope are more intensive in the Gr catchment than in the Gn and Se catchments.

Table 1. Mean baseline inventories of  $^{137}\text{Cs}$  within soils in Korea

Location area	Baseline (Bq/ m <sup>2</sup> and Bq/kg)	Authors	Year
Granite	48.10 Bq/g	Cho <i>et al</i>	1994
Tuff	773.0 Bq/g	Cho <i>et al</i>	1994
Daejon area	14.37 Bq/kg	Lee <i>et al</i>	1995

Forest land	2501 Bq/m <sup>2</sup>	Lee, <i>et al</i>	1998
Hills	1058 Bq/m <sup>2</sup>	Lee, <i>et al</i>	1998
Paddy field	17.70 Bq/kg	Choi <i>et al</i>	1999
Upland field	27.80 Bq/kg	Choi <i>et al</i>	1999
Gr1 catchment (Uijongbu)	2100 Bq/m <sup>2</sup>	This study	2005
Gr2 catchment (Seoul)	2222 Bq/m <sup>2</sup>	This study	2005
Gn catchment (Yangsurri)	2840 Bq/m <sup>2</sup>	This study	2005
Se catchment (Yeongcheon)	3366 Bq/m <sup>2</sup>	This study	2005

[O-2]

## The expansion of gully in the mountainous slope, South Korea

JIN-KWAN KIM<sup>1</sup>, DONG-YOON YANG<sup>1</sup>, MIN-SEOK KIM<sup>1</sup>, SANGHEON YI<sup>1</sup>

<sup>1</sup>Korea Institute of Geoscience and Mineral Resources, Korea ([jkkim@kigam.re.kr](mailto:jkkim@kigam.re.kr))

The information related the processes of sediment generation and transportation in catchment that causes seriously damage to life and property is a significant to manage catchments and to frame a policy. Specially, the changes in artificial land-use accelerate soil erosion and slope failure. Morphometric changes on the mountainous slope associated with construction of some graves developed obviously gullying around Godam-dong in Icheon-Shi during about last five years. And competition between oaks and Japanese larch for limited nutrients is the primary cause of the low stature and finally Japanese larch is died out in the study area.

Gully expansion with gully-bed erosion, side-wall failure and head-wall retreat induced by surface flow and subsurface flow, generally, occurs. According to previous studies, the factors of gully expansion have been known by heavy rainstorm, freeze-thaw effect during the winter season, piping flow and etc., and the control factor of that has also been known by representatively the effect of plant root. Therefore, we have performed the geodetic survey, the soil-profile analysis and direct shear test, and have monitored the pore-water pressure on gully to find out the growing mechanism of the gully from September 2004 to February 2006.

The head wall of gully retreated approximately 1.3 m and the depth at the point of gully head retreat was about 0.7m from October 2004 to October 2005. And the side wall of gully near the tensiometers collapsed, thus, the width of gully at the point of side-wall collapsing expanded about 1.3m. From October 2005 till February 2006, there was not the expansion of gully on the surface, however, the sedimentation on the gully bottom occurred from about 5 to 30cm depth. The

sediment of gully-bed fell off the exposed root mat where perched on the upper gully-wall, but root mat was not collapsed. Therefore, from the seasonal gully change point of view, during the winter season, the freeze-thaw effect led to the soil detachment from the exposed root mat, thus, the detached sediment laid on the lower gully-wall and gully-bed. During the summer season, the flow induced by rainstorm within gully led to transport sediment and collapse the gully-wall.

Specially, the large expansion of gully occurred mainly by heavy summer rainstorm on 11-12 August 2005. During this period, total rainfall was about 135.5mm, and this precipitation was one of the most rainfall events during the monitoring period, however, the frequency of 135.5mm rainfall was annual recurrence according to result from the rainfall frequency analysis. For 11-12 August 2005, especially, gully expansion occurred near the tensiometers, at this time, tree fell down over the tensiometer sensor. According to tensiometer data, slope stability was going to be stable when tree went down. Consequently, considering the slope stability and the characteristic of tree in the study area, we suggest that the side-wall failure of gully occurred during the heavy rainfall period was caused by the process that the temporary flow within gully undercut the gully side-wall where the soil shear strength was reduced by weaken root, and then the tree and root mat where perched on the upper gully-wall collapsed.

[O-3]

### **Difference in Surface Erosion in Granite, Gneiss and Sedimentary rock Catchments**

YUKIYA TANAKA<sup>1</sup>, ORKHONSELENGE ALEXANDER<sup>1</sup>, SONG-HYUN KIM<sup>1</sup>

<sup>1</sup>*Department of Geography, Kyunghee University, Korea (ytanaka@khu.ac.kr)*

In order to measure soil loss along the hillslopes and sediment discharge, field experimental plots were established on downslopes, 27-32 degree slopes with granite (Gr1, Gr2), gneiss (Gn) and sedimentary rock (Se) catchments. The plots were located according to uniform slope steepness and on smooth surfaces with natural vegetation. Monitoring of plots extended over a six month period from April to October, 2005. Plot surface areas (10.5m<sup>2</sup>) were defined by two sidewalls of 3m length, one upper wall of 3 m length and the lower triangular apron contact. The walls were made of about 20cm high damp plastic cloth. The floor of the triangle was excavated to a 20cm depth under the soil surface and a plastic collecting drum was half buried and connected to the pipe. At the apex of apron, a 60cm internal plastic pipe was inserted to convey water and surface sediment in the



approximately 45 liter sediment collector drum. Sediment yields were collected manually from the 10.5cm<sup>2</sup> surface areas by brushing into plastic container drums every month after substantial rainfall. Sediments were analyzed through a dry sieve (above 0φ) and organic matter was determined by loss on ignition at 550°C over 4 hours. In the plots, rainfall intensity was measured with a recording rain gauge. The runoff was measured by specially designed pre-calibrated flumes, equipped with water-depth probes. Sediment yields in plots were calculated from periodic sediment samples taken throughout the hydrograph. As a result of measurement from four erosion plots, high discharge and sedimentation were shown to be markedly associated with the occurrence of heavy rainfall events. The treatment effects on erosion rates were very obvious depending on difference of bedrocks. The highest discharge and surface erosion were generated in Gr1 and Gr2 catchments, whereas discharge and surface erosion were not generated in the Se catchment during the observation period. The highest sedimentation rate occurred at 1.21 g/l due to heavy rainfall event on June 27 in Gr1 catchment. In July and August, the highest sedimentation occurred in Gr2 catchment, where sedimentation rates were 0.26 g/l and 0.12 g/l, respectively. In Gn, the surface erosion and sedimentation were almost not generated during the observation period. However, a sediment discharge occurred as a result of extremely heavy rainfall event on August 11. The Se had no occurrence of surface soil erosion and sedimentation during the observation period. This indicates that the surface soil has low soil erodibility by surface flow during heavy rainfall. Generally, in terms of soil erosion and sedimentation rates compared to the other plots, the Gr2 had highest erosion and sedimentation rates in July and August. The highest sedimentation on the plot surface was revealed in the Gr1 and Gr2 catchments, which have less dense vegetation cover in the plot surface area than in the other catchments. This indicates the influence of soil surface compacting effects produced by heavy rainfall. The soil cover in The Gr1 and Gr2 catchments had higher erosion rates due to high rainfall erosivity and higher exposure of the surface soil to heavy rainfall events than in the Gn and Se rock catchments.

[O-4]

**Investigating infiltration rate, erosion rates and erosion processes within a Japanese cypress plantation using Cs-137 and Pb-210ex measurements**

YUICHI ONDA<sup>1</sup>, TAIJIRO FUKUYAMA<sup>2</sup>, SHUN ITO<sup>1</sup>, HIROAKI KATO<sup>1</sup>, MARINO HIRAOKA<sup>1</sup>,  
CHISATO TAKENAKA<sup>3</sup>

<sup>1</sup>*Graduate School of Life and Environmental Sciences, University of Tsukuba, Japan  
(onda@atm.geo.tsukuba.ac.jp)*

<sup>2</sup>*National Institute of Agro-Environmental Sciences, 3-1-3 Kannondai, Tsukuba, Ibaraki 305-8604, Japan*

<sup>3</sup>*Graduate School of Bioagricultural Sciences, Nagoya University, Furo-cho, Chikusa, Nagoya 464-8602, Japan*

The In Japan, soil erosion represents an important threat to the longer-term sustainability of Japanese cypress plantations. Although it has been demonstrated that raindrop impact, rather than sheet or rill/gully erosion, is the dominant process in both sediment detachment and sediment transport at the point or slope scale in such plantations, the role of overland flow in sediment production at the catchment scale has received little attention to date. In order to identify the dominant erosion process operating in Japanese cypress plantation catchments, we measured infiltration rate using a oscillating nozzle-type infiltrometer and monitored the sediment yield in small plot (2 x 5m) and watershed schale (3600m<sup>2</sup>). We also simulated the sediment transport capacities of both overland flow, expressed as a function of the upslope contributing area, and local slope gradient, rainsplash, expressed as a function of the local slope gradient and the kinetic energy of the rainfall. In addition, we compared the simulation results with the erosion rates estimated using Cs-137 and Pb-210<sub>ex</sub> measurements undertaken at each sampling point. The infiltration rate in unmanaged Japanese cypress plantation was found to be 14-39 mm/h. Using this value the simulated local transport capacity of overland flow indicated a close correspondence with the local erosion rates estimated using the radionuclide measurements. In contrast, there was no significant correlation between the simulated rainsplash transport and the local erosion rates estimated from the radionuclide measurements. These results suggest that overland flow makes a significant contribution to surface soil erosion even on forested hillslopes. These results demonstrate the potential for using Cs-137 and Pb-210<sub>ex</sub> measurements to produce independent information on long-term soil erosion rates, which can be used for investigating erosion processes and validating erosion models.

[O-5]

## **Behavior of As in low crystalline iron oxide during the alteration process in acid mine drainage environments**

KEISUKE FUKUSHI<sup>1</sup>, MORIO TAKADA<sup>2</sup>, KEN-ICHI ITO<sup>2</sup>, TSUTOMU SATO<sup>2</sup>

<sup>1</sup>*Institute of Nature & Environmental Technology, Kanazawa University, Japan*

[fukushi@kenroku.kanazawa-u.ac.jp](mailto:fukushi@kenroku.kanazawa-u.ac.jp)

<sup>2</sup>*Course of Sustainable Resources Engineering, Faculty of Engineering, Hokkaido University, Japan*

## **INTRODUCTION**

In this workshop held at Daejeon, Korea (2004), we reported the natural attenuation of As in drainage at an abandoned As mine area. In this area, As in the drainage is scavenged by authigenic schwertmannite (low crystalline iron oxide containing sulfate). Schwertmannite is metastable phase with respect to crystalline iron oxide such as goethite (Bigham et al., 1996; Yu et al, 1999). In order to estimate the long-term stability of natural attenuation process of As during the sedimentation process, it is essential to understand the behavior of As during the schwertmannite alteration. In present study, the natural precipitates are characterized mineralogically to gain some clues for understanding the behavior of arsenic during the alteration. In addition, As (V) adsorption experiments on synthesized schwertmannite and alteration experiments of As(V) adsorbed schwertmannite were conducted in order to reveal the effect of adsorbed As on alteration of schwertmannite and the molecular scale behavior of arsenate in schwertmannite. Moreover, by using estimated parameters from these laboratory experiments, we carried out 1-dimensional reactive transport modeling to understand the lifetime of schwertmannite and long-term efficiency of natural attenuation of As in acid mine drainage environments.

## **SAMPLES AND METHODS**

The pH, ORP, electric conductivity and temperature of drainage water were measured on site. The concentrations of dissolved components were measured by ICP-mass and ion-chromatography. Collected precipitates were characterized by X-ray diffraction (XRD). The precipitates were dissolved by 6M HCl, and resulting solutions were analyzed by ICP-mass to determine Fe and As content. In some collected samples, a banded structure with brownish and yellowish colors was observed on a millimeter scale. Fractions from each layer were collected and analyzed by XRD and infrared spectroscopy. Selective extraction technique was applied for each fraction and the chemical form of As are estimated from the distribution of As in the phase extracted using the ICP-MS.

Adsorption of As (V) by schwertmannite was examined as a function of As (V) concentration at a constant ionic strength ( $I = 0.01$ ). The pH of the solutions was adjusted to 4 by addition of conc. HNO<sub>3</sub>. After 24 hours of reaction at 25°C, the pH of the suspensions was measured and the suspensions were filtered. The solutions were served for the analyses of Fe, As and SO<sub>4</sub>. After the As (V) adsorption experiments, the prepared As(V) adsorbed samples were aged in electrolyte

solutions ( $I = 0.01$ ) with  $\text{pH} = 4$  at 30, 50 and 70°C for 200 days. A portion of suspensions were periodically sampled, filtered, characterized by XRD to determine the alteration and served for TAO extraction to quantify the amounts of remained schwertmannite after aging.

## RESULTS AND DISCUSSION

XRD of natural precipitates showed that the precipitates consist of schwertmannite and goethite. According to Bigham et al. 1996 and Yu et al. 1999, schwertmannite is a direct product from solution and goethite forms via alteration of schwertmannite in acid mine drainage conditions. The As contents in the precipitates usually exceeds 30mg per g of dried samples. XRD analyses of each fraction from banded structures of the precipitates showed that brownish parts are rich in schwertmannite while yellowish parts are rich in goethite. Selective extraction procedure showed that As contents are well correlated with iron content derived from schwertmannite. On the other hand, As contents in yellowish parts are significantly low compared with brownish parts. These results from selective extraction imply that schwertmannite processes significant adsorption capacity for As while goethite does not. Alteration experiments of As (V) adsorbed schwertmannite indicated that transformation rate of schwertmannite which contains significant amount of As (V) ( $85\text{mg}\cdot\text{g}^{-1}$ ) is two order magnitude lower than that of As free schwertmannite at 25°C. The occurrence of banded structures in the precipitates may be explained by the differences of the transformation rates. The brownish schwertmannite would remain when the amount of As adsorption is sufficient to retard the transformation rate. In contrast, when the amount of As adsorption is insufficient, the brownish schwertmannite would transform to the yellowish goethite.

The results of adsorption experiments showed that schwertmannite released 0.62 mmol of  $\text{SO}_4^{2-}$  for every 1 mmol of  $\text{H}_2\text{AsO}_4^-$  and 0.24 mmol of  $\text{OH}^-$  that has been adsorbed. As (V) replaces  $\text{SO}_4$  up to the half of total  $\text{SO}_4$  in schwertmannite. The equivalent exchange relationship indicated that arsenic adsorbed schwertmannite would behave as a solid solution between schwertmannite containing maximum amount of As (V) and As (V) free schwertmannite. The equilibrium constant for the anion exchange in solid solution reaction, estimated from the reacted solution chemistries, showed that thermodynamic stability of schwertmannite containing maximum amount of As(V) is significantly higher than that of As free schwertmannite. The solid solution reactions would explain the stabilization of schwertmannite by adsorbing As observed in natural condition.

1-dimensional reactive transport modeling in acid mine drainage conditions quantitatively suggests that As (V) adsorbed schwertmannite remain significantly large period compared with As free schwertmannite. This indicates that As (V) adsorption makes the schwertmannite more stable and a long-term effective As (V) sink in natural conditions. Moreover, the results imply that

schwertmannite could serve for the excellent remediation material for the environmentally degraded areas by As.

## REFERENCES

- Bigham, J.M., Schwertmann, U., Traina, S.J., Winland, R.L., Wolf, M., (1996) GCA. 60, 2111-2121.
- Yu, J., Heo, B., Choi, I., Cho, J., Chang, H., 1999. GCA. 63, 3407-3416.

## [O-6]

### **Palynofloras evidence for historical state of the Golden Crown Gaya (3-7<sup>th</sup> centuries AD) in the Gimhae fluvial plains, Southern Korean Peninsula**

SANGHEN YI<sup>1</sup>, DONG-YOON YANG<sup>1</sup>, JU-YOUNG KIM<sup>1</sup>, SUN YOON<sup>2</sup>

<sup>1</sup>*Korea Institute of Geoscience and Mineral Resources, Korea (shyi@kigam.re.kr)*

<sup>2</sup>*Department of Geology, Pusan National University, Korea*

This paper presents the results of studies of palynomorphs recovered from two cores collected near the Yeanri burial mound on the Gimhae fluvial plain. Two local pollen zones were recognized on the basis of variations in the palynofloral assemblage: a lower Pollen Zone I (*Pinus-Quercus* assemblage), and an upper Pollen Zone II (*Pinus-Quercus-Gramineae* assemblage). Pollen Zone I is further subdivided into a lower Pollen Zone Ia (*Pinus-Quercus-Taxodiaceae* assemblage) and an upper Pollen Zone Ib (*Pinus-Quercus-Pterocarya* assemblage). Based on the palynological analysis, the depositional environments changed from marine to non-marine before 1280±110 <sup>14</sup>C yr B.P. Pollen Zone Ia is typical of a lower intertidal flat of a shallow bay environment, whereas Pollen Ib is characteristic of an upper intertidal flat in a shallow bay. Pollen Zone II is typical of a fluvial plain similar to that of today. An environmental change may have resulted from increased sediment discharge of the Nakdong River. Afterward, an exposed area was modified by human activities, as indicated by a sudden increase in grassland herbaceous pollen grains. Palynological data, combined with paleontological data and historical literature, provide a better understanding of the history of Golden Crown Gaya State and the reason why it eventually merged with the Shilla State.

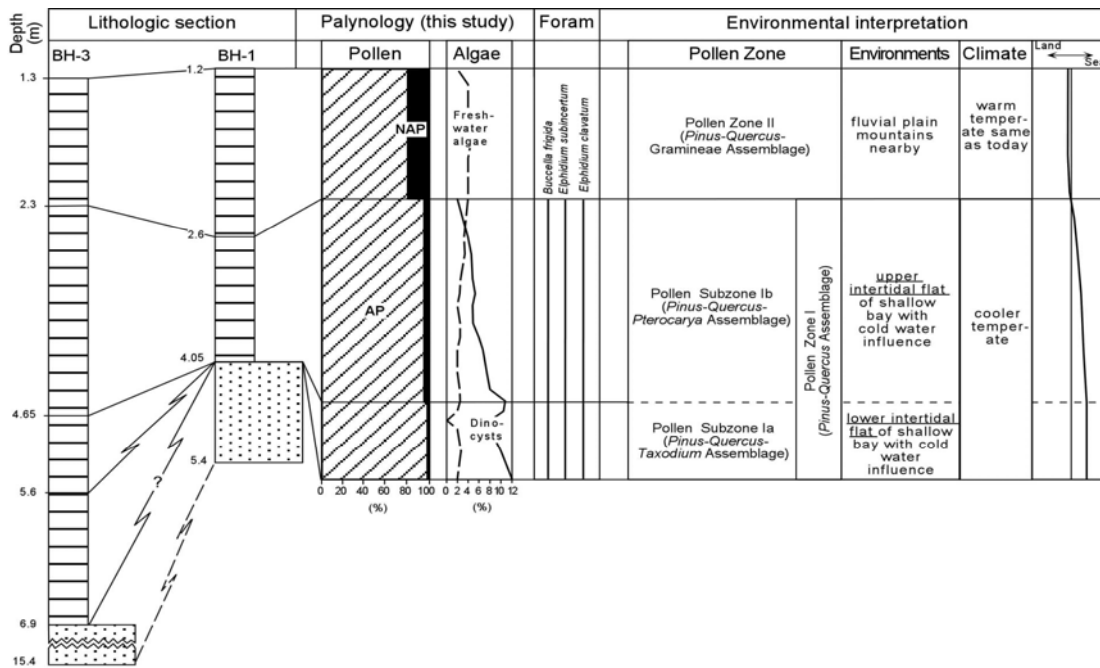


Fig.1. Correlation between two cores with local palynological assemblage zones recognized showing environmental interpretations.

[O-7]

## Limnological response to climate changes over the past 200 yr in Namu Co, central Tibet

XIANGDONG YANG<sup>1</sup>

<sup>1</sup>Key Laboratory of Lake Sediment and Environment, Nanjing Institute of Geography and Limnology, Chinese Academy of Sciences, 210008 Nanjing, China (xdyang@niglas.ac.cn)

Namu Co is the largest alpine lake in Tibet, with the meltwater-fed from the valley glaciers of western Nianqingtanggula Mountain. Sediment analysis of independent grain-size and fossil diatoms from a short core in the west part of the lake have been employed to reconstruct the variations in water inflow and lake salinity in order to understand the limnological responses to the climate changes and its influenced glacial activities over the past two centuries. The diatom-inferred water conductivity shows Namu Co was once a freshwater with freshwater *Aulacoseira ambigua* dominate during the last cold interval of the Little Ice Age (LIA). Water conductivity has increased since 1870 and presented a rapid increasing trend in the recent 40 years, with the marked shift in dominant diatoms from *Cyclotella ocellata* to *Staphanodiscus minutulus* towards the top sediment

core. However, the progressive enhanced meltwater inputs after the LIA recorded by the gradual increases of median grain size and coarser fractions to the up core show an inverse relation to lake salinity. The consistence in changes between diatom-inferred conductivity and the instrumental temperature measurements in the recent 40 years suggests that temperature is the main factor strongly influencing the hydrological balance of the lake through the evaporation, hence resulting in the changes of lake salinity, as well as lake-level fluctuations and lake effective moisture. In addition, by the comparisons among lakes with and without melt-water supply along the section from southern to northern Tibet, the synchronous hydrological changes in lakes with different salinity were found, revealing the common responses of inland lakes to regional climatic changes and further illustrating the important role temperature plays in driving the lake hydrological balance in regional scale, albeit the strong glacier recession could maintain the lower salinity in Nam Co and other glacier-fed lakes such as Yangzhuoyong Co and Chen Co in the last century especially in the recent decades. This study also reveals the cold-wet and warm-dry environment patterns in Tibetan region in at least century scale.

[O-8]

## **Diatom record of the Late Quaternary in the East/Japan Sea**

EUNYOUNG RYU<sup>1</sup>, SEONG-JOO LEE<sup>1</sup>, DONG-YOON YANG<sup>2</sup>, JU-YONG KIM<sup>2</sup>

<sup>1</sup>*Department of Geology, Kyungpook National University, Daegu, 702-701, Korea ([ryu415@chol.com](mailto:ryu415@chol.com))*

<sup>2</sup>*Korea Institute of Geoscience and Mineral Resources, Daejeon 305-350, Korea*

Diatom assemblages in the East/Japan Sea core sediments have been used frequently as quantitative predictors of environmental parameters such as sea surface-water temperature, salinity, influx and circulation of the Tsushima Warm Current and eustatic sea-level changes.

The East/Japan Sea based on marine diatoms is very sensitive and unique environment. The Tsushima Warm Current has an important affect on controlling the distribution and composition of diatom flora, which in turn, reveal the history of the Tsushima Warm Current in this area. The typical indicators of the Tsushima Warm Current, *Pseudoeunotia doliolus*, first appeared in East Sea at 10 ka and shortly found during Late Quaternary. This indicates that at least 3-4 short warm period existed in the late Pleistocene. The high abundance of *P. doliolus* and warm water diatoms at the base of core 00GHP-01 suggest that a strong inflow of Tsushima Warm Current into the East/Japan Sea. It might be indicative of the last interstadial, around MIS 5e (125,000 yr BP). During the Last Glacial Maximum, the East/Japan Sea was nearly isolated from the surrounding seas because of the eustatic low sea-level, and was covered with low-salinity water. Salinity

decreased due to increased freshwater input from rivers draining the surrounding lands. A large peak of the *Paralia sulcata* reflects influx of large amount of terrestrial material and the influence of the low salinity water supplied from the Korean peninsular. It is interpreted that the lower salinity was caused by the glacioeustatic drop in sea level and a relative reduction of the influx of Tsushima Warm Current increased supply of freshwater to the East/Japan Sea.

[O-9]

## **Nutrient sources and paleoproductivity during the past century in Longgan Lake, middle reaches of Yangtze River, China**

YANHONG WU<sup>1,2</sup>, ANDREAS LÜCKE<sup>2</sup>, SUMIN WANG<sup>1</sup>

<sup>1</sup>*Nanjing Institute of Geography and Limnology, Chinese Academy of Sciences, Nanjing 210008, People's Republic of China*

<sup>2</sup>*Institute of Chemistry and Dynamics of the Geosphere V: Sedimentary Systems, Research Center Jülich, D-52425 Jülich, Germany*

Total organic carbon (TOC), total nitrogen (TN), total phosphorous (TP) and isotope ratios ( $^{13}\text{C}_{\text{Org}}$ ,  $^{15}\text{N}$ ) were measured in a 63 cm lake sediment core from Longgan Lake, middle reaches of Yangtze River, China. These geochemical and isotopic records provide a continuous history of recent variations of lake productivity and trophic state. After Suess-effect correcting,  $^{13}\text{C}_{\text{Org}}$  together with TOC, TN and TP, indicated that during the last century, the primary productivity of Longgan Lake increased continuously and trophic state evolved from oligotrophic to mestrotrophic. Anthropogenic source of organic carbon (OC), nitrogen (N) and phosphorous (P) were distinguished from their natural backgrounds, which suggested that the enhancing of human activity in lake catchment since 1950s, especially the utilization of artificial fertilizer, increased the input of OC, N and P. The lake productivity hence was elevated by the excess nutrients, resulting in the increase of  $^{13}\text{C}_{\text{Org}}$  (corrected).  $^{15}\text{N}$  of bulk sediments did not show increase trends with the productivity elevated which might be resulted from the input of nitrogen from chemical fertilizer.

Key words: Organic carbon, phosphorous, isotopic ratio, anthropogenic source, lake productivity, Longgan Lake, China



## Seasonal Change of Particulate Matter Transport and Vertical Water Mixing Processes with Climatic Changes in Lake Biwa

YASUAKI AOTA<sup>1</sup>, KENJI KASHIWAYA<sup>2</sup>, MICHIO KUMAGAI<sup>3</sup>

<sup>1</sup>*Institute of Nature and Environmental Technology, Kanazawa University, Kakuma, Kanazawa, Ishikawa 920-1192, Japan (yaota@kenroku.kanazawa-u.ac.jp)*

<sup>2</sup>*Institute of Nature and Environmental Technology, Kanazawa University, Kakuma, Kanazawa, Ishikawa 920-1192, Japan*

<sup>3</sup>*Lake Biwa Environmental Research Institute, 5-34 Yanagasaki, Otsu, Shiga 520-0022, Japan*

Seasonal change of sediments collected from the trap at the North Basin of Lake Biwa was considered. We carried out the sediment trap experiment from the early 2003, and continuous monitoring of water currents and temperature from the middle of 2003. In this workshop, we report monthly trend of sediments, water movements in the lake and some climatic data.

From the past studies on the southern slope of the North Basin of Lake Biwa, re-suspension of the lake bottom due to strong wind was observed for several hours during the stratified season, and the enhancement of the upward transport of the sediments was suggested. Indeed, heavy rain may enhance the inflow of the particles into the lake through river and several pathways, and may affect the amount of particle transport around the lake. These results in the past studies suggest that relatively short-term (daily) climatic changes might affect sedimentation processes in the lake bottom environment. From the monthly study for four years, it was observed that the thickness of high turbid layer around lake bottom was increased after heavy rain. In this study, they deduced that organic matter such as phytoplankton produced near the lake surface might sustain the high turbid layer around the lake bottom during the stratified season through its settlement. However, the mechanisms and climatic factors affecting the seasonal changes in the lake sediments are still unclear.

The sediments in the trap are a total amount of particles transported through both processes, where its origin came from re-suspension of the particle from lake-bottom (internal factor) or transport of the particle from catchment of the lake (external factor). Therefore, we need to clarify these factors affecting seasonal change of the sediments. Water currents have not been measured so much in the deep layers of Lake Biwa as in the shallow layers. However, several observational studies in the deep layers of the lake reported the existence of the relatively strong currents (10-15cm/s), and vertical flux of the sediments in the lake bottom might be enhanced.

In this workshop, we show monthly trend of sediments, water movements in the lake obtained from water current and temperature observation, and discuss the sedimentation processes for a monthly or relatively short time-scale with water movements and climatic changes.

## **Environmental records for recent decades in Jinheung Pond sediments (Jeongeup, Jeollabukdo, Korea)**

WOOK-HYUN NAHM<sup>1</sup>, GYOO HO LEE<sup>2</sup>, DONG-YOON YANG<sup>1</sup>, JU-YONG KIM<sup>1</sup>, KENJI  
KASHIWAYA<sup>3</sup>

<sup>1</sup>*Korea Institute of Geoscience and Mineral Resources (KIGAM), Korea (nahmwh@empal.com)*

<sup>2</sup>*Department of Earth System Sciences, Yonsei University, Korea*

<sup>3</sup>*Institute of Nature and Environmental Technology, Kanazawa University, Japan*

This paper describes the mean grain-size and heavy metal data of the <sup>137</sup>Cs-dated BS-3 sediment core (35 cm long) recovered from Jinheung Pond, located in the southwestern part of the Korean Peninsula. Grain-size analysis of Jinheung Pond shows a clear climate signal. Instrumental records of annual rainfall and excess 50 mm rainfall (annual summation of the excess of more than 50 mm per day), which are reflecting the energy available for sediment transport, correlate well with the mean grain-size distributions measured from the BS-3 core. The most plausible mechanism for this response in mean grain-size is variation in the annual amount and intensity of precipitation. Increase or decrease in precipitation potentially produces the effect of increased or decreased sediment inflow, and consequently causing the larger or smaller grain-size, respectively.

Massive economic growth and agriculture development in the area of Jinheung Pond started only from the early 1990s. The heavy metals including Cd, Pb, Cu, and Zn tend to increase from 8 cm depth toward the core top. This enrichment may reflect the impacts of human-derived contaminant inputs from recent development around the pond.

The results of this study make the sediments of Jinheung Pond highly suitable for further past and future environmental investigations with a very high time resolution.

## **U and Th Isotopes in Lake sediments, Lake Biwa system in Japan: To obtain Insight into Their Paleoenvironmental Implications**

AYA SAKAGUCHI<sup>1</sup>, MASAYOSHI YAMAMOTO<sup>1</sup>, JUMPEI TOMITA<sup>1</sup>, HISAKI KOFUJI<sup>2</sup>, YASUAKI  
AOTA<sup>3</sup>, KI-ICHIRO YOKOTA<sup>4</sup>, MICHIO KUMAGAI<sup>4</sup>

<sup>1</sup>*Low Level Radioactivity Laboratory, Kanazawa University, Japan ([aya-s@llrl.ku-unet.ocn.ne.jp](mailto:aya-s@llrl.ku-unet.ocn.ne.jp))*

<sup>2</sup>*Japan Marine Science foundation, Japan*

<sup>3</sup>*Department of Earth and Environmental Science, Kanazawa University, Japan*

Many studies have revealed that lacustrine sediments in continental interior provide a continuous records of physical, chemical and biological changes within the lake, and processes in the lake's watershed which have reflected the continental climate, corresponding to multiple glacial-interglacial cycles. The clearest signals of changed paleoclimate in the Lake Baikal sediments are the number of diatom frustules (or biogenic silica), and organic carbon content. Microelements, especially uranium (U), have also been noticed as one of the most important chemical indexes in Lake Baikal. The U increases during periods of warmer climate coincide well with the number of diatom frustules (or biogenic silica content) and give us an important tool to reconstruct the paleoenvironmental changes. Recent study suggested that little U exist in the diatom frustules, and scavenging of U in water column is governed by not only the difference for adsorption capacity of suspended particles but also the speciation of U depending on the alkalinity in water. Furthermore, we have to consider about the amount of U supply from watershed to the lake. Thorium isotopes in sediments provide useful information on history as an independent proxy for terrestrial materials and on chronological tool.

Fundamental studies on U and Th isotopes (<sup>238</sup>U, <sup>234</sup>U, <sup>230</sup>Th and <sup>232</sup>Th) in lake system are, therefore, very important to deepen our understanding on their sedimentary and sedimentation behaviors, chronology using <sup>234</sup>U-<sup>238</sup>U and/or <sup>230</sup>Th-<sup>238</sup>U methods and linkage to environmental changes. In this study, Lake Biwa system in Japan was used as a research field, and river and lake waters, suspended materials, sediment trap samples and bottom sediments from the lake have been measured for U and Th isotopes. Some other parameters of water and sediments were also measured. The purpose of this study was to obtain the information on sedimentary behaviors of U and Th isotopes to the lake bottom and to obtain insight into their implications for paleoclimatic change.

Lake Biwa is the largest freshwater lake in Japan with two basins; northern and southern basins. Thermal stratification occurs in the northern basin from May to December. It has more than 100 input rivers and its outflow is only Seta River. The sampling sites are shown in Fig. 2. Water samples were collected seasonally (1993-2000) and monthly (Jul. 2004 - ) from some depths of the lake. Riverine water samples (18 rivers) were taken and monthly samples collected continuously from the Rivers Ane and Ado. These were immediately filtrated by 0.45- m membrane filter and U contents and <sup>234</sup>U/<sup>238</sup>U activity ratios (A.R.) of each fraction (filtrate and particulate) were determined by ICP-MS or -ray spectrometry after chemical separation. Temperature, pH, conductivity, alkalinity and major anion and cation, etc. were also measured in these samples. Cylindrical sediment traps were employed in the water depth of ca. 35 m and 85 m at an offshore River Ado in the lake (water depth: ca. 90 m. July 2004-). These monthly sediment-trap samples

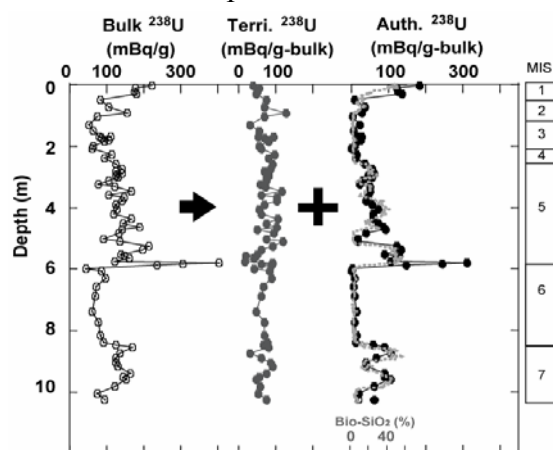


Fig. 1. Depth distributions of authigenic, terrigenous and bulk (total) <sup>238</sup>U fractions and biogenic silica content in the core from Academician Ridge, Lake Baikal.

were freeze-dried and measured for some radionuclides ( $^{210}\text{Pb}$ ,  $^{234}\text{Th}$ ,  $^7\text{Be}$ ,  $^{137}\text{Cs}$ , etc.) by  $\alpha$ -ray spectrometer. The samples were also treated with diluted acid (0.1M HCl in 5%  $\text{H}_2\text{O}_2$ ) for 30min in  $80^\circ\text{C}$  water-bath. The leachate and residue were measured for U and Th isotopes by ICP-MS or  $\beta$ -ray spectrometer after chemical separation. Zooplankton and phytoplankton were also monthly collected from surface lake water with 22  $\mu\text{m}$  pore size plankton-net to find out the bioaccumulation of U by primary products.

Dissolved U concentration of river and lake water were found in wide ranges of 0.003- 1.3 mBq/L and 0.09- 0.38 mBq/L, respectively, reflecting the sampling points (and/or depth) and seasons. Typical depth profiles of U contents in lake water are shown in Fig. 3 along with the water temperature. The depth profiles of  $^{238}\text{U}$  concentration are almost constant during the circulation period (Dec.-Apr.), but during the stratific periods,  $^{238}\text{U}$  concentration in surface layer becomes high. In deep layer,  $^{238}\text{U}$  contents decrease abruptly during the stratific period. Thus, the variation of  $^{238}\text{U}$  in lake water is controlled by both  $^{238}\text{U}$  supply from rivers and its removal from deep layer during the stratific period. The residence time of  $^{238}\text{U}$  in the lake was estimated to be ca. 3 years from the mass balance of  $^{238}\text{U}$ . Its value, ca. 3 years, compared with a water residence time of 5.5 years, indicates its affinity for particles. The sedimentary behaviors of  $^{238}\text{U}$  will be discussed along with data set of suspended particles sediment-trap samples and lake bottom sediments.

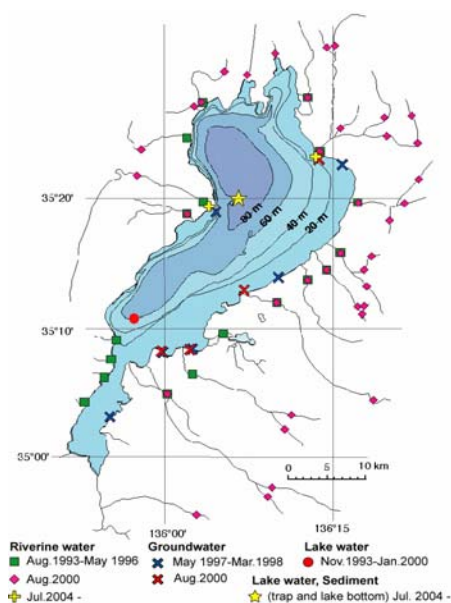


Fig.2 Sampling locations and event periods in Lake Biwa system.

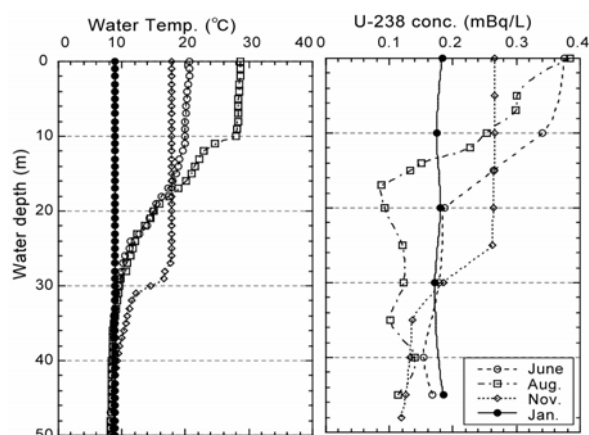


Fig. 3 Typical depth profiles for seasons of water temperature and  $^{238}\text{U}$  contents in lake water.

## Uranium-series Disequilibrium Application to Lake Sediments in Geochronology - A Short General Review -

MASAYOSHI YAMAMOTO<sup>1</sup>, AYA SAKAGUCHI<sup>1</sup>, JUNPEI TOMITA<sup>1</sup>

<sup>1</sup>Low Level Radioactivity Laboratory, K-INET, Kanazawa University, Japan (pluto@llrl.ku-unet.ocn.ne.jp)

Now, it has become very important to get information about the past and present environmental changes to predict the future climatic changes caused by natural and artificial events. Terrestrial sediments, especially, lacustrine sediments give us an opportunity to understand the paleoenvironmental changes in continental interior, compared with polar ice and deep-sea sediments unsusceptible of the local effects. Reconstruction of the paleoenvironmental changes has been attempted with appropriate approaches by using physical, chemical and biological signatures inferred from the lake sediments. In this case, it is indispensable to establish a chronology for reading quantitative historical information from the sediment records. Until now, many radiometric and non-radiometric dating methods have been developed. As far as radiometric dating techniques are concerned, the following methods have been mainly applied to the dating of sediments: <sup>210</sup>Pb·<sup>137</sup>Cs (present – ca 150 yr), <sup>14</sup>C (a few 1000 yr – ca. 30 kyr), uranium-series disequilibrium (ca.10 kyr - several 100 kyr), <sup>10</sup>Be·<sup>26</sup>Al (a few 100 kyr – several 10 Myr ) and so on.

In the fields of archaeology, Quaternary geology and geomorphology, the ability to date events in the time interval of about 5 kyr to 500 kyr BP is of vital importance. Uranium-series dating is known to be the most successful methods applied to this interval, and has commanded much attention and effort. Among the many uranium-series disequilibrium applications, <sup>234</sup>U/<sup>238</sup>U and <sup>230</sup>Th/<sup>234</sup>U(or <sup>238</sup>U) dating methods have been employed and successfully applied to the dating of clean carbonate precipitates such as corals and speleothems (cave-deposited travertines). Usually, these materials fill the following important requirements for U-series dating: (1) The sample remains a closed system. (2)When formed, the sample does not contain <sup>230</sup>Th (in case of Ionium dating) and its <sup>230</sup>Th all originates from subsequent *in-situ* decay of <sup>238</sup>U and <sup>234</sup>U.

However, the applications of these methods to lake sediments have been limited because of the unsurety about assurance for closed system of sediment layer after the burial of settling particles from the water column. Furthermore, the main problem involves the presence of detrital materials which can not be isolated from sediments by simple physical means. In other words, its presence makes the estimation of “authigenic” U and Th fractions difficult. No physical means is available to completely separate the detritus from the sediment matrix. There have been various attempts made to cope with the detrital materials contamination problem. A common approach adopted to achieve this is leaching using diluted HCl or HNO<sub>3</sub>, and then, after isotopes analyses of U (<sup>238</sup>U, <sup>234</sup>U) and Th (<sup>232</sup>Th, <sup>230</sup>Th) in both the leachate and residue, correction is made for the detrital contamination to determine “authigenic” <sup>238</sup>U, <sup>234</sup>U and <sup>230</sup>Th, i.e., <sup>234</sup>U/<sup>238</sup>U and <sup>230</sup>Th/<sup>234</sup>U ratios,. The acid-leaching method using isochron approaches has been used to date lacustrine marls, halite, tufa, fossil snails, evaporatic deposits, sulphate minerals, lacustrine carbonates (gastropods, ostracods) and carbonate sediments. On the other hand, when bulk sediments are used, <sup>232</sup>Th has been often

used as a correction index to estimate “authigenic”  $^{238}\text{U}$ ,  $^{234}\text{U}$  and  $^{230}\text{Th}$ . This approach makes assumption that secular equilibrium exists in the detrital minerals (i.e.,  $^{238}\text{U} = ^{234}\text{U} = ^{230}\text{Th}$  in terms of activity).

Here, we review several approaches using  $^{234}\text{U}/^{238}\text{U}$  and  $^{230}\text{Th}/^{234}\text{U}$  (or  $^{238}\text{U}$ ) dating methods which could be applied to lake sediments.

1. Mean sedimentation rate (Fig.1, using our data).
2. Dating using isochron approach (Fig. 2, by Zhibang et al.)
3. Dating using quasi-isochron approach (Fig. 3, by Goldberg et al.)

Finally, it must be kept in mind that diagenesis and post-depositional effects such as dewatering, compaction, bioturbation and chemical changes are ignored in these methods. Therefore, agreement should be obtained for ages determined by several independent methods.

Authigenic  $^{234}\text{U}/^{238}\text{U}$ ,  $^{230}\text{Th}/^{238}\text{U}$ : R1, R2  
 $R1 = 1 + (R_0 - 1) \times \text{Exp}(-\lambda_4 \times D/S)$   
 $R2 = 1 - \text{Exp}(-\lambda_0 \times D/S) + (R_0 - 1) \times \lambda_0 / (\lambda_0 - \lambda_4) \times (R_0 - 1) \times \text{Exp}(-\lambda_4 \times D/S) \times \{1 - \text{Exp}(-\lambda_0 \times D/S + \lambda_4 \times D/S)\}$   
 Mean sedimentation rate:  $4.47 \pm 0.37$  cm/kyr

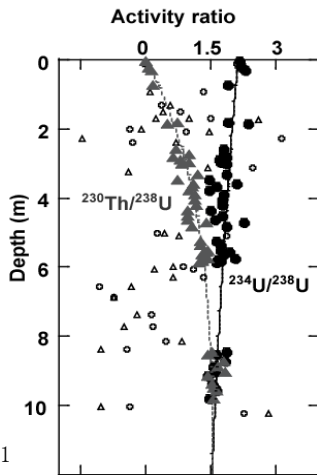


Fig. 1

Depth distributions of authigenic U-234/U-238 and Th-230/U-238 activity ratios in the sediment core. Circles are U-234/U-238 and triangles Th-230/U-238. Solid symbols are for all data and open symbols for selected data excluding glacial periods. By using U-234/U-238 and Th-230/U-238 dating methods, the data with data from cold intervals excluded were fitted using non-linear optimization techniques to obtain the mean sedimentation rate.

A0, A4, A8 and A2: Measured activities of Th-230, U-234, U-238 and Th-232.

Ab = U-238/Th-232 ratio in clastic material

$$A4/A2 = A8/A2 + q(A8/A2 - Ab) \exp(-\lambda_4 t)$$

$$A0/A2 = Ab + (A8/A2 - Ab) \{1 - \exp(-\lambda_0 t) + qf\}$$

$$A0/A2 = a(A4/A2) + b$$

$$a = (A0/A2 - Ab) / (A4/A2 - Ab)$$

$$= [1 - \exp(-\lambda_0 t) + qf] / [1 + q \exp(-\lambda_4 t)]$$

Fig. 3 Quasi-isochron using narrow interval of sediment core. This method was applied to dating of the last two interglacials in sediments from Lake Baikal by Goldberg et al. (2001).

$$^{230}\text{Th}_A = ^{230}\text{Th}_L - (^{230}\text{Th}_R / ^{232}\text{Th}_R) \times ^{232}\text{Th}_L$$

$$^{234}\text{U}_A = ^{234}\text{U}_L - (^{234}\text{U}_R / ^{232}\text{Th}_R) \times ^{232}\text{Th}_L$$

$$^{238}\text{U}_A = ^{238}\text{U}_L - (^{238}\text{U}_R / ^{232}\text{Th}_R) \times ^{232}\text{Th}_L$$

$$\frac{^{230}\text{Th}_A}{^{234}\text{U}_A} = \frac{(^{230}\text{Th}_L / ^{232}\text{Th}_L) - (^{230}\text{Th}_R / ^{232}\text{Th}_R)}{(^{234}\text{U}_L / ^{232}\text{Th}_L) - (^{234}\text{U}_R / ^{232}\text{Th}_R)}$$

$$\frac{^{234}\text{U}_A}{^{238}\text{U}_A} = \frac{(^{234}\text{U}_L / ^{232}\text{Th}_L) - (^{234}\text{U}_R / ^{232}\text{Th}_R)}{(^{238}\text{U}_L / ^{232}\text{Th}_L) - (^{238}\text{U}_R / ^{232}\text{Th}_R)}$$

$$^{230}\text{Th}_A / ^{234}\text{U}_A = ^{238}\text{U}_A / ^{234}\text{U}_A [1 - \text{Exp}(-\lambda_0 T)] + \lambda_0 / (\lambda_0 - \lambda_4) \times (1 - ^{238}\text{U}_A / ^{234}\text{U}_A) \times [1 - \text{Exp}(-\lambda_0 + \lambda_4) T]$$

L and R show the leachate and residue fractions

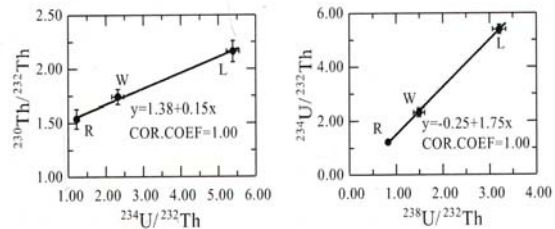
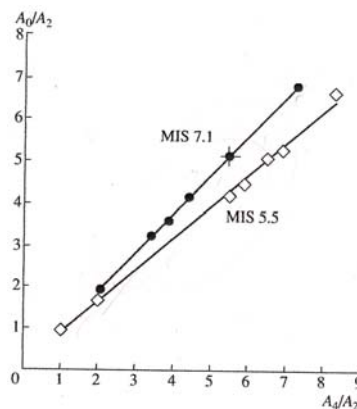


Fig. 2. Dating using isochron approaches



Two typical quasi-isochrons of sediments at Station 15 for intervals of 491–523 cm (MIS 5.5) and 739–760 cm (MIS 7.1). MIS 5.5:  $R = 0.75 \pm 0.013$ ; age  $132 \pm 4$  ka;  $A_b = 0.47 \pm 0.27$ . MIS 7.1:  $R = 0.916 \pm 0.17$ ; age  $202 \pm 9.7$  ka;  $A_b = 0.35 \pm 0.93$ .

## Development of 2D FEM algorithm for bed elevation change in a curved channel

TAE BEOM KIM<sup>1</sup>, SUNG-UK CHOI<sup>1</sup>, KYUNG DUCK MIN<sup>2</sup>

<sup>1</sup>*School of Civil & Environmental Engineering, Yonsei University, Korea ([geo108@naver.com](mailto:geo108@naver.com))*

<sup>2</sup>*Department of Earth System Sciences, Yonsei University, Korea*

Most natural streams or rivers are sinuous or meandering. The flow characteristics and the sediment transport mechanism are more complicated in a curved channel than the straight one. There is centrifugal acceleration in a curved channel which reaches a maximum value near the water surface. Therefore, the outer bank water surface is overburdened in a transversal cross section. To satisfy the mass conservation, water in the lower layers moves in the inward direction. When this secondary flow circulation combines with the primary flow motion in the longitudinal direction, it generates a complex 3D helical or spiral motion. The inward motion near the channel bed transports sediments from the outer bank towards the inner bank. So the scour and deposition occur in the outer bank and in the inner bank, respectively.

The purpose of this study is development of 2D FEM model which is capable of predicting the time variation of the bed elevation change in a morphologically variable channel including curved one. The shallow water equations and the Exner's equation are solved with FEM. For validation, developed model is applied to 180° curved channel. The simulated results show deposition near the inner bank and erosion near the outer banks, which agree well with the measured data. In order to validate boundary condition algorithm, developed model is applied to the case of inflow of overburdened upstream sediment load. Comparisons are made between experimental data and simulated results. This is based on the decoupled model approach and restricted to uniform sediment, so neglecting armoring or grain sorting effects.

## Lake-Catchment System and Kosa-covering Area in East Eurasia

KENJI KASHIWAYA<sup>1</sup>

<sup>1</sup>*Institute of Nature and Environmental Technology, Kanazawa University*

Fundamental solutions for the many global environmental issues have to be searched for considering conservation of the ecosystem and diversity of species, and harmony of sustainable human existence. Especially, in Asia, an area anticipating/expecting a population explosion, it is

essential to improve precision and resolution of predictions and estimates, and thereby to strengthen the international cooperation through exchange of information and environmental management strategies. The existence of highly reliable, high-resolution chronological information becomes a major premise. In the mid-latitude regions of East Asia, there exists many written records dating back thousands of years, including authentic Chinese history, and the 472-year history of the 25 successive reigns of Choson Dynasty (1392-1863) recorded chronologically in the “Annals of the Choson Dynasty,” (registered by UNESCO World Heritage in 1997). Further, there also exist the oldest, longest preserved, high resolution terrestrial records of loess sediment of the Chinese Loess Plateau and lacustrine sediment from Lake Baikal extending tens of millions of years into the past, far exceeding known human history. In other words, in this region there remain all the essential records for study of the environmental process (closely related to sustainable development and human existence), and all the necessary proxy records of long-term environmental change for discussion on ecology and the diversity of species.

It is comparatively easy to obtain detailed data and literature regarding climate and meteorological phenomena related to every aspect of environment for the modern period of instrumental observation. As a result, it is possible to discuss the many aspects of global environmental changes in the period. Further, it has gradually become possible to predict future changes. However, significant limitations still remain. One such problem is the limitation of sequential documentation and data, both chronological and spatial. Currently most detailed discussions on future predictions are based on quantitative data of the instrumental observation period. These data mainly cover the period of warming after the Little Ice Age. However, it is also necessary to clarify earth surface responses to environmental changes in different climate regimes such as the Medieval Warm Period and the Little Ice Age for future environmental predictions because some changes in the current climatic regime have to be considered for future environmental conditions. Observed quantitative data available for these periods are limited (probably precipitation data in the Choson Dynasty of Korea are only). Hence, we need proxy data for the periods as well as other climatic regimes. When considering present global warming, continuous quantitative environmental (climatic) data are indispensable for discussions on artificial, human factors before and after the industrial revolution. Then, what kind of proxy data can be used to obtain this continuum of information including the interval? Generally, most data used until now are common to long-term environmental analysis; tree rings (dendrochronology), marine sediment, ice cores, lacustrine sediments, aeolian sediments, etc. Most proxy data found in the kosa-covering regions including the Japan Sea area can be utilized, but when considering responses to each terrestrial phenomena including bio-activity, lake sediments are ideal in the view point of resolution



and continuity. From the perspective of lake-catchment system, analysis of lake sediments also contributes to understanding catchment processes and becomes essential in clarifying environmental processes.

From the perspective of prediction and estimation of environmental change, and environmental management strategies, detailed knowledge is required of the response of the earth's surface system (including the human domain) to external environmental changes; understanding temporal changes in the environment and environmental processes is indispensable. This becomes essential to understanding the environmental processes. "Lake-catchment" system is a possible system combining environmental processes with temporal environmental changes (recorded in lake sediments).

Changes in the physical environment of the earth's surface, for example, due to external forces such as heavy rain falls or earthquakes, bring about such responses as topographic changes; soil erosion, land slides, etc. which relate to the mass movement and sediment discharge. It is well-known that environmental changes are recorded in lake or reservoir sediments when there are some lakes or reservoirs in the down stream. In a semi-closed system, such as a "lake-catchment system", the relationship between the changes in the physical environment within the catchment and lake sediment records is often very clear. Especially, when the system is instrumentally observed, the above relationship becomes causally clearer. Then, sediment records become an effective clue to clarify phenomena within the catchment (environmental processes). This is the first important step to combine observational information with paleo-records beyond observational limit.

For example, mathematical expressions for physical environmental conditions in the lake-catchment system will be introduced here for further discussions. Material moved per unit time in the catchment is:

$$dM_i/dt = F(C_i(t), D_i(t))$$

with  $M_i$ ; volume of material moved in the  $i$ -th region (catchment),  $C_i$ ; climatic factor in the  $i$ -th region,  $D_i$ ; catchment factor in the  $i$ -th region. Here,

$$C_i(t) = f_{ci}(T_i, P_i, W_i) \text{ with } T; \text{ temperature, } P; \text{ precipitation and } W; \text{ wind, and}$$

$D_i(t) = f_{Di}(G_i, B_i, L_i)$  with  $G$ ; topography factor,  $B$ ; vegetation factor and  $L$ ; land use factor.

Sedimentation rate ( $dV_i/dt$ ) in the lake is proportional to the material moved;

$$dV_i/dt = \lambda dM_i/dt,$$

where  $\lambda$  is proportional factor. Mass depth ( $H$ ) per unit area is expressed;  $H = \rho V_i/A$ , then

$$dH/dt = \rho\lambda/A F (C_i(t), D_i(t))$$

with  $\rho$ ; sediment density and  $A$ ; lake floor area. This is a relationship between (mass) sedimentation rate and catchment environment. Therefore,

$$H(t) = \rho\lambda/A \int_{t_0}^{t_f} F (c_i(t), D_i(t)) dt$$

[O-16]

## Historical Records of Asian Dust Events (Hwangsa) in Korea

YOUNGSIN CHUN<sup>1</sup>

<sup>1</sup>*Hwangsa Research Team/ Meteorological Research Institute, 460-18, Sindaebang-dong, Dongjak-gu, Seoul 156-720, Korea (yschun@metri.re.kr)*

The observation of dust events in Korea must have been important through its long history due to its geographical and meteorological setting. Description about dust events was well documented in historical archives, such as Samguk sagi (BC 57 - AD 938), Goryeo sa (918-1392), Joseon wangjosillok (1392-1853) and Munhuenbigo (~ 1776). In this study, records of Asian dust events were reconstructed from the above historical archives, covering the period of the 2<sup>nd</sup> ~ 18<sup>th</sup> century. These historical records were investigated along with the recent data (1914–2004) of dust event days in Seoul, Korea.

The first record was made in AD 174 in Silla during the period of the Three Kingdoms. Dust event, now called Hwangsa, was commonly written down as “Woo-Tou” standing for dustfall in historical archives. Although there might be a chance for retrieved data to be biased by several factors such as socio-political instability, the main seasonal feature of the historical dust events was found to be in good agreement with that of the last 90 years. Asian dust events took place most frequently during spring from March to May and there was no occurrence in summer. Therefore, it is likely that the extracted data adequately reflect dust events in Korea over historical times.



(TOU)

(WOO)

Figure 1 The symbolic word standing for dustfall and description of how each letter was shaped. The first syllable, “Tou(土)” symbolizes the shape of small plant emerging from the earth or soil and the second, “Woo(雨)” represents the motion of raindrops falling down from a cloud.

[O-17]

## Detection of Yellow Sand Dust from multiple satellite measurements

JHOON KIM<sup>1</sup>, JAEHWA LEE<sup>1</sup>

<sup>1</sup>IEAA BK21 Program, Global Environment Lab., Dep. of Atmos. Sci., Yonsei University, 134 Sinchon-dong, Seodaemoon-gu, Seoul 120-749, Korea (jkim2@yonsei.ac.kr)

Aerosol affects the Earth’s climate by scattering and absorbing radiation and by altering the cloud microphysics. Since these effects are different from one type to the other, aerosol type detection from satellite remote sensing is important. Aerosol also affects human health and industrial activity. Especially, dust type aerosol can cause human disease and affect significant portion of high-tech electronic industrial production including semiconductor. This study shows temporal and spatial distribution of four major aerosol types (dust, carbonaceous, seasalt and sulfate) retrieved by MODIS-OMI algorithm [cf. Jeong and Li, 2005] and 4-channel algorithm [Higurashi and Nakajima, 2002] from Moderate Resolution Imaging Spectroradiometer (MODIS) and Ozone Monitoring Instrument (OMI) data over the East Asia. The consistency of the aerosol type classification from two different algorithms also presented.

Retrieved results show that there exist complex types of aerosol over the East Asia from emitted and transported sources. Dust type aerosol often occurred mixed with carbonaceous type aerosol. It implies that the dust type aerosol is loaded and transported with polluted air mass. The evidence of long distance transportation of polluted air mass is also captured, that is, over the remote ocean area, not only seasalt type aerosol but also sulfate type aerosol is detected. In general, two different algorithms produce reasonably consistent results. The agreement of absorptance and size of the aerosol retrieved from two different algorithms is over 70% and 80% respectively and types of the aerosol is nearly 60% during springtime of East Asia. The agreement is better for non-absorbing aerosol than absorbing one, and is better for fine mode than coarse mode. Dust type aerosol detected from satellite agrees reasonably well with the SPRINTARS and ground observation results over the East Asia.

[O-18]

## **Simulation of East Asia Climate Change for the Last Glacial Maximum**

SEONG-JOONG KIM<sup>1</sup>, BANG YONG LEE<sup>1</sup>

<sup>1</sup>*Korea Polar Research Institute, KORDI, Korea (seongkim@kopri.re.kr)*

### **1. Introduction**

Ice core records have shown that the global climate fluctuate from glacial to interglacial with 100,000 year periods for the last 0.5 million years. It is believed that the climate fluctuations are due to the periodic variation of earth's orbital parameters (Hays et al., 1976). The Last Glaciation occurred at 20,000 years ago and this time is called the Last Glacial Maximum (LGM). According to CLIMAP (1981), the global mean sea surface temperature was about 5°C lower in the LGM than at present with a small temperature change in the low latitudes and a large change in the high latitudes. There was an expansion of ice sheet over North America and northern Europe with an height of 1,500-2,000 m and the sea ice expanded to 50°S in the southern hemisphere and 45°N in the North Atlantic.

Many geological and geochemical proxy data are used to depict the climate change pattern of the LGM, these have limitations in describing the climate change mechanism. Besides proxy data, numerical models have been used to investigate the climate change for the past and present. In order to understand the climate change mechanism of the LGM, many classes of numerical models have been used (Gates, 1976; Manabe and Hahn, 1977; Kutzbach and Guetter, 1986, Weaver et al., 1998; Ganopolski et al., 1998; Hewitt et al., 2001; Kim et al., 2002, 2003). However, because these models are composed of low spatial resolutions, they have limitation in simulating regional-scale

climate features such as East Asia. In this study, we used a relatively high-resolution climate model and investigate the climate change of East Asia for the LGM.

## **2. Model and experiments**

The simulations were performed with the Community Climate Model version 3 (CCM3) atmospheric general circulation model at about 75 km with 18 vertical levels. The CCM3 includes a comprehensive model of land surface processes known as the NCAR Land Surface Model (LSM). Important physical processes are represented as described in detail by Duffy et al. (2003).

Two experiments are analyzed. The modern climate simulation, referred to as MOD, is forced by climatologically-averaged monthly sea-surface temperatures (SSTs) and sea ice distributions provided by NCAR, a specified CO<sub>2</sub> concentration of 355 ppm, and present land mask and topography. The second experiment features glacial boundary conditions. Over ocean the SST and sea ice are prescribed using climatologically averaged monthly data prepared with the August and February reconstructions by the CLIMAP (1981). The glacial surface topography was modified following the Ice-4G reconstructions and the land mask is modified to account for the lower sea level (~120 m). The atmospheric CO<sub>2</sub> concentration is reduced to 200 ppm following ice core data. Vegetation and soil types are unchanged except over glaciated surfaces. Land points arising due to sea level reduction are assigned a medium soil type. Orbital parameters set to 20k BP.

## **3. Results**

The modern experiment reproduces the climate features reasonably well in comparison to observations. For example, in winter there is a remarkable temperature reduction over land in comparison to surrounding seas due to the lower heat capacity. This feature is well represented in the modern simulation (Fig. 1). On the other hand, in summer the land is heated faster, the temperature over land is higher.

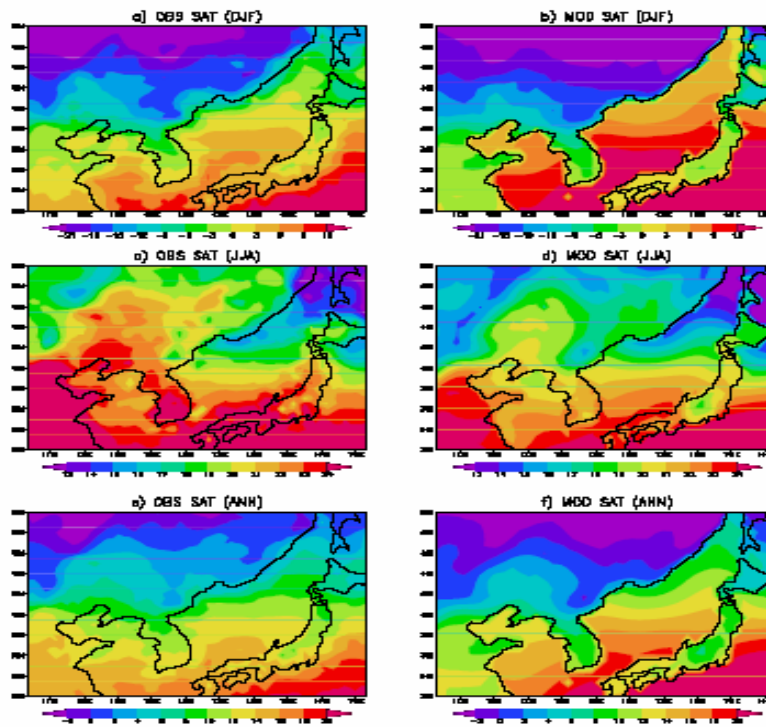


**Fig. 1** Geographic distribution of observed surface air temperature (SAT) for a) winter (December-January-February), c) summer (June-July-August), e) annual-mean, simulated in the MOD for b) winter, d) summer, f) annual-mean.

Under LGM boundary conditions, surface temperature is markedly reduced by more than  $18^{\circ}\text{C}$  in the Korean west sea and continental margin of the Korean east sea, where the ocean exposed to land in the LGM, whereas in these areas surface temperature is warmer than present by up to  $2^{\circ}\text{C}$  (Fig. 2). This is due to the difference in heat capacity between ocean and land. Overall, in the LGM surface is cooled by  $4\sim 6^{\circ}\text{C}$  in northeast Asia land and by  $7.1^{\circ}\text{C}$  in the entire area. An analysis of surface heat fluxes show that the surface cooling is due to the increase in outgoing longwave radiation associated with the reduced  $\text{CO}_2$  concentration.

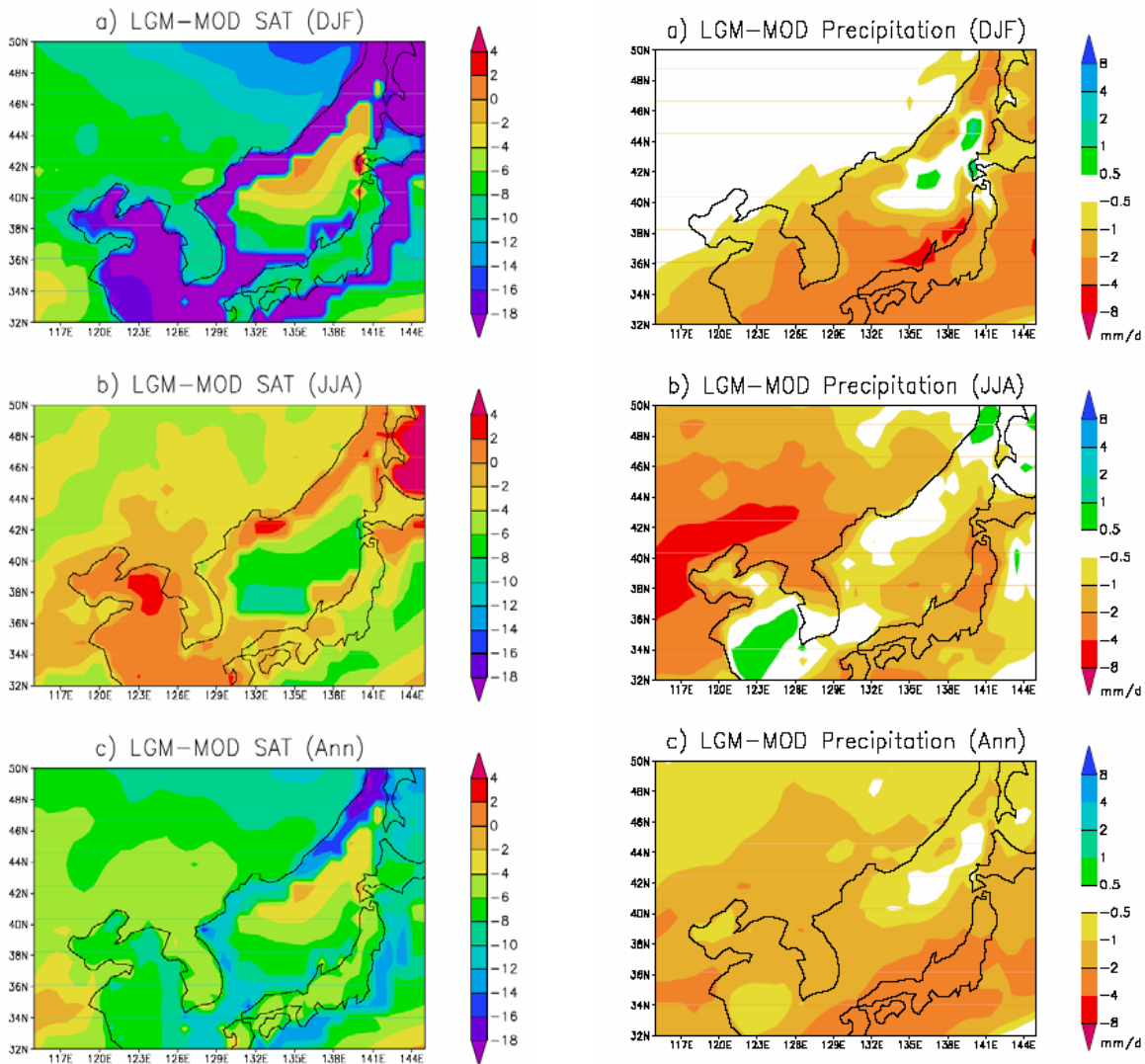


**Fig. 2** Geographic distribution of the change in SAT for a) winter, b) summer and c) annual-mean.

**Fig. 3** Geographic distribution of the change in precipitation for a) winter, b) summer, c) annual-mean. Units are in  $\text{mm day}^{-1}$ .

The reduction in surface temperature leads to a weakening of the hydrological cycle. In winter, precipitation decreases largely in the southeastern part of Asia by about 1~4 mm/day, while in summer a larger reduction is found over China (Fig. 3). Overall, annual-mean precipitation decreases by about 50% in the LGM. In northeast Asia, evaporation is also overall reduced in the LGM, but the reduction of precipitation is larger, eventually leading to a drier climate. The drier LGM climate simulated in this study is consistent with proxy evidence compiled in other areas.

In conclusion, the high-resolution model captures the climate features reasonably well under global domain.

**Acknowledgement** This study was supported by the project “Polar Atmospheric Composition and Climate Change (PE06030)” of Korea Polar Research Institute and “Asian Monsoon Simulation Study (PG05020)” of KORDI.

## References

- CLIMAP, 1981, Seasonal reconstructions of the Earth's surface at the last glacial maximum, Geol. Soc. Amer. Map Chart Ser., MC-36.
- Duffy, P.B., Govindasamy, B., Iorio, J.P., Milovich, J., Sperber, K.R., Taylor, K.E., Wehner, M.F. and Thompson, S.L., 2003, High-resolution simulations of global climate, part 1: present climate, *Clim. Dyn.*, 21, 371-390.
- Ganopolski, A., Rahmstorf, S., Petoukhov, V. and Claussen, M., 1998, Simulation of modern and glacial climates with a coupled global model of intermediate complexity, *Nature*, 391, 351-356.
- Gates, W.L., 1976, Modelling the Ice-Age climate, *Science*, 191, 1138-1144.
- Hays, J.D., Mobrie, J.I. and Shackleton, N.J., 1976, Variations in the earth's orbit: pacemaker of the ice ages, *Science*, 158, 1121-1132.
- Hewitt, C.D., Broccoli, A.C., Mitchell, J.F. and Stouffer, R.J., 2001, A coupled model study of the last glacial maximum: Was part of the North Atlantic relatively warm? *Geophys. Res. Lett.*, 28, 1571-1574.
- Kim, S.-J., Flato, G.M., Boer, G.J. and McFarlane, N.A., 2002, A coupled climate model simulation of the Last Glacial Maximum, Part 1: Transient multi-decadal response, *Clim. Dyn.*, 19, 515-537.
- Kim, S.-J., Flato, G.M. and Boer, G.J., 2003, A coupled climate model simulation of the Last Glacial Maximum, Part 2: approach to equilibrium, *Clim. Dyn.*, 20, 635-661.
- Kutzbach, J.E. and Guetter, P., 1986, The influence of changing orbital parameters and surface boundary conditions on climate simulations for the past 18000 years, *J. Atmos. Sci.*, 43, 1726-1738.
- Manabe, S. and Hahn, D.G., 1977, Simulation of the tropical climate of an ice age, *J. Geophys. Res.*, 82, 3889-3911.
- Weaver, A.J., Eby, M., Fanning, A.F. and Wiebe, E.C., 1998, Simulated influence of carbon dioxide, orbital forcing and ice sheets on the climate of the last glacial maximum, *Nature*, 394, 847-853.

[O-19]

## Five Years of Monsoonal Record in the Soda Straw of Seopdong Cave, Korea

KYUNG SIK WOO<sup>1</sup>, KYOUNG NAM JO<sup>1</sup>

<sup>1</sup>*Cave Research Institute of Korea, Kangwon National University, Chuncheon, Kangwondo 200-701, Korea*



Limestone caves are extensively developed in Gangwondo and Chungcheongbukdo (Korea) and more than 1000 caves are estimated to be present. A variety of numerous speleothems are actively growing in these caves today. One soda straw which has been growing in Seopdong Cave, Kangwondo, Korea, was investigated to use as East Asian Monsoon recorder. Monsoonal climatic variations can be detected from the soda straw which grew for five years (July, 1999 ~ July, 2004). This soda straw is ca. 20 cm long, indicating that its growth rate is 4 cm/yr. Excess  $^{210}\text{Pb}$  variation coincides well with the amount of precipitation during its growth, and the values are high during rainy summers and low during dry winters. This indicates that radioactive-decayed  $^{210}\text{Pb}$  incorporated into rainwater reached the cave very rapidly due to the short transit time of rainwater into the cave.

Oxygen and carbon isotopic compositions of the soda straw are  $-8.6 \sim -7.7$  and  $-7.8 \sim -5.8$  per mil (PDB), respectively. These values show that the calcite in soda straw precipitated in oxygen isotopic equilibrium. Carbon isotope contents are relatively more depleted from 2000 to 2001, and this was probably due to the smaller amount of rainfall during this interval. It is believed that the smaller amount is reflected by more depleted  $\delta^{13}\text{C}$  values, because degassing rate of  $\text{CO}_2$  decreases with decreasing supply rate of cave water from overlying limestone. On the contrary, the periods of higher precipitation (1999, 2002~2004) show more enriched  $\delta^{13}\text{C}$  values. The overall trend suggests that  $\delta^{13}\text{C}$  of soda straw should be controlled by the degassing rate of  $\text{CO}_2$ . Higher degassing rate can be confirmed by higher partial pressure of  $\text{CO}_2$  (1500 ppm) of cave atmosphere during summer, and lower pressure (430 ppm) during winter. Three different trends of elemental variations can be observed in the soda straw: 1) La, Zr and Y shows strong linear correlation with overall rainfall trend, 2) Ba, Sr, U and Mn show inverse correlation, and 3) P only shows the quantitative changes of annual rainfall. Especially, the second group indicates the distinctive peaks only during the periods of low annual precipitation. High-resolution geochemical signals recorded in the soda straw of Korean limestone cave may promise a great potential for the reconstruction of climate and environmental changes during the last hundred or thousand years or so.

[O-20]

### **The origin of erratic calcite speleothems in the Dangcheomul Lava Tube, Jeju Island, Korea**

JEONG CHAN KIM<sup>1</sup>, KYEONG SIK WOO<sup>2</sup>, DON WON CHOI<sup>1</sup>, JIN KYEONG KIM<sup>2</sup>, DONG YOON  
YANG<sup>1</sup>

<sup>1</sup>*Korea Institute of Geoscience and Mineral Resources, 30 Gajeong-dong, Yuseong-gu, Daejeon, 305-350, Korea*

<sup>2</sup>*Cave Research Institute of Korea, Kangwon National University, Chuncheon, Kangwondo 200-701, Korea*

Dangcheomul Cave is a lava tube in the volcanic terrane of Jeju Island, Korea. The cave is located only a few meters below the surface under alkali basalt and shows typical lava tube morphology and internal microtopographic features as can be seen in many other lava tubes elsewhere. In spite of its lava-tube origin, lava tube speleothems such as lava stalactites are relatively rare, except for abundant lava helictites on the ceiling which have the same chemical composition as the surrounding basalt. Rather, this cave is a lime-decorated lava tube characterized by well-developed carbonate speleothems such as soda straws, stalactites, stalagmites, columns, cave corals, curtains, flowstones, rimstones, carbonate powders, and shelfstones.

Carbonate sand dunes overlying the lava tube are responsible for the formation of the calcite speleothems. The sand dunes were formed from the carbonate sediments transported from adjacent shallow seas and beaches, and are composed of mollusks, echinoderms, coralline algae, benthic foraminifers, bryozoans, etc. Oxygen isotopic compositions of some speleothems and cave water indicate that the speleothems have grown mostly by evaporation of seepage water. Also, carbon isotopic compositions suggest that the majority of carbon was derived from overlying carbonates with a minor contribution of organic carbon from soil.

Most speleothems in Dangcheomul Cave do not show typical morphology as can be commonly seen in limestone caves. These erratic forms result from a combination of 1) the penetration of plant roots from the overlying soil into the cave, 2) the supply of meteoric water along the roots, and 3) precipitation of carbonate minerals around the roots. Geochemical analyses indicate that evaporation of cave water rather than degassing of carbon dioxide played an important role in the formation of calcite speleothems.

[O-21]

## **Paleosols Sequence of Last Glacial Maximum of South Korea**

JU-YONG KIM<sup>1</sup>, DONG-YOON YANG<sup>1</sup>, WOOK-HYUN NAHM<sup>1</sup>, SEI-SUN HONG<sup>1</sup>, JEONG-CHAN KIM<sup>1</sup>, JIN YOUNG LEE<sup>1</sup>, JIN-KWAN KIM<sup>1</sup>, KEUN-CHANG OH<sup>1</sup>, DON-WON CHOI<sup>1</sup>

<sup>1</sup>*Korea Institute of Geoscience and Mineral Resources, Korea (kim@kigam.re.kr)*

In South Korea Last Glacial Paleosol Sequence are found at a number of paleolithic sites along river basins and in the coastal areas. These paleosols are assumed to be derived from many cycles of seasonally freezing and thawing process, which can be detected as frost cracks in the periglacial soil-sedimentary profiles. The soil-landscape forming process of the Last Glacial period of South Korea is typified by both polygonal structures in plan view, and ground veins or frost cracks (or soil wedges in local name) associated with foliation textures in vertical view. This soil type can be found as active phenomena in the East Siberia, i.e., Olhon Island of Baikal Lake. The vertical length of frost cracks in many Korean soil-sedimentary profiles ranges from several tens of decimeter up to several meters. Clay fillings and coating in the cracks are prevailed and materials are derived from surrounding matrix. This soil type associated with frost cracks and foliation textures are named as the Last Glacial Paleosol, and it is representative of a pedostratigraphic term designating one of the upper paleolithic cultures of South Korea. Two paleosols are distinct in Korea. The upper paleosol shows dark pinkish brown loams with relatively stiffer than paleosol below. The filled materials along upper vertical cracks are continuous, lightly yellow to pale bluish gray towards top, but it turns into discontinuous and dark reddish brown at lower part of the profile. The microscopic texture shows many clay cappings, patches of aggregates of Fe-Mn hydroxides, and a number of clay fills and translocation along the silty interstices and cracks. Lastly the radiocarbon ages of this typical paleosol indicate cold period of Last Glacial Maximum, approximately as old as 18~22Ka.



Fig. 1 Paleosol of Last Glacial Maximum, showing cryoturbation, polygonal structure and fragipan (Donghae city).

# **A Climate Change in the Tumen River Basin**

AI-FEN JIN<sup>1</sup>

<sup>1</sup>*Department of Geography, Science College of Yanbian University, Yanji, 133002, China*

This paper studied the Climate change of the Tumen River basin over the past 50 (1953-2002) years . The results show that the air temperature in the Tumen river basin has several significant inter-annual oscillation periods, namely 8-year period, 3-4 year period and quasi-biennial oscillation (QBO). The 3-4-year oscillation is mainly associated with ENSO and always leads the variation of ENSO inter-annual variability signal. QBO is related to the variation of the Indian Ocean-monsoon system and the East Asian trough, which is always shown as a maximum lag correlation. There still exists a long-term tendency and an obvious abrupt climate change that occurred in 1972 in the time series of the Tumen River basin air temperature. After 1972, the anomalous annual mean temperature rose from -0.35 °C before its abrupt change to 0.68 °C . The temperature fell before 1972 and rose remarkably after 1972, but the total trend shows an upward tendency from 1953 to 2002. The result about precipitation analysis from annual time series shows that the precipitation has several significant inter-annual oscillation periods, namely 3-year period, 4 year period and 7 year period. The result from monthly time series shows that the precipitation has 3-month period and 2.8 month period。 Quasi 3 month period oscillation is most strong signal in the middle of the Tumen River basin.

[O-23]

## **The natural surroundings of Yanbian Area**

CHUN-JING LI<sup>1</sup>

<sup>1</sup>*Department of Geography, Science College of Yanbian University, Yanji, China*

### **I. General situation**

Yanbian Area refers to the Yanbian Korean Autonomous Prefecture, which belongs to the Changbai mountain system, North East China. It is located at between 41°59'47"and 44°30'42"N, and 127°27'43" and 131°18'33"E. The total area is 42.7000square kilometers. The whole area consists of mountain area, hilly land and basin area. There are 27 mountains whose breeze height is

above 1000 meters in Changbai Mountain, which gets through the whole Yanbian Area.. Among them the highest one is White Cloud Breeze with 2691-meter-high elevation. Plains are mostly river valley, and there are four main rivers such as Tumen River, Shonghua River, SuifenRiver and Mudan River. Among them the Tumen River is the most important one, which takes up 22.632square kms of the whole Tumen River area and 53% of the total area of Yanbian. The Tumen River rises in the main breeze, DongLu of Changbai Mountain, which has 1.290-m total drop and whose average slope is 1.2%. The main tributaries in the side of China are, from the upper reaches, HongqiRiver, HailanRiver, BuerhatongRiver, GayaRiver and HunchunRiver.

## II. Topographic characteristics and classification of agriculture +based on DEM in Yanbian Area

In this paper, Topographic characteristics such as elevation, relief and slope etc. in Yanbian area are analyzed quantitatively with Arc GIS soft ware. The result shows that average elevation of Yanbian Area is 691.8m, and the average slope angle is 7.91°.The area of sloping towards the centre from four ways are distributed well ,with some height and gentle slope. From the analysis of the accumulative curve of area measure ratio by elevation, Yanbian Area, view the situation a whole, takes on uneven topography, as is convex in low elevation, a little straight in middle elevation and obviously uneven in high elevation. It shows that Yanbian Area belongs to the old terrain development stage. From the different height area ratio, we can see the area ratio under 300-m elevation and above 1500-m elevation is fairly low, while most area is centered between 300-1500m height. In Yanbian Area there is little large smooth area, nor is high and steep mountain area. Most area consists of plateau and platform. From the distributed different relief area ratio, we can see the relief in Yanbian Area is mainly centered between 5-15°. And there is hardly any area higher than 25°, which is useful for land use and the regional development plan.

## III. Analysis the characteristics of Tumen River system according to its main tributaries

In this paper, characteristics of river system such as drainage-basin shape, plane shape of river system, density of drainage network, bifurcation ratio of the river, and bend coefficient of the river etc. are analyzed quantitatively by the GIS based on vector 1:5 river system map in Tumen River basin. The result shows that the plane shape of each tributary of Tumen River is mostly the system of bifurcation: Density of the drainage network is between 0.29~0.7. Bend coefficient of mainstream is between 1.12 (slight) ~ 3.40 (complicated), and the drainage-basin shape is elliptical, which is between ellipse (E=0.6)~close to ellipse (E=0.919). The average bifurcation ratio is between 3.32~4.396. All these show that the impacts of geological structure on the drainage-basin are not so obvious.

## Progress in research on lake culture eutrophication in East China

SUMIN WANG<sup>1</sup>, XIANGDONG YANG<sup>1</sup>, YANHONG WU<sup>1</sup>, JINGLU WU<sup>1</sup>, JIAN LIU<sup>1</sup>

<sup>1</sup>*Key Laboratory of Lake Sedimentation and Environment, Nanjing Institute of Geography and Limnology, Chinese Academy of Sciences, Nanjing, 210008, P. R. China (smwang@niglas.ac.cn)*

Forced by human activity, 70% of lakes in East China have suffered from expeditious eutrophication, which is threatening water resources security and human health, and becoming the focus attracting attentions from the governments and scientists. Approaches of biology, geochemistry, statistics and numerical simulation have been widely used to quantitatively distinguish anthropogenic contribution to lake eutrophication. Based on the regional database of diatom and chironomid, the transfer function between diatom, chironomid, and total phosphorous (TP) of lake water may be established, then the evolution sequence of TP in lake water can be reconstructed by fossil diatom and chironomid in lacustrine sediments, natural nutrient background and ecological response to trophic level can be analyzed and determined, finally the potential threshold of trophic level for lake eutrophication can also be diagnosed. Based on the relationships between nutrient elements (C, N and P) and referent elements (Al, Fe, Ti, etc.) in lake sediments, the natural flux of nutrients accumulation in lake catchment can be obtained, and then anthropogenic portion can be estimated with the strengthening human activities. The comparisons of the long term integrated climatic simulation results of Model Echo-G, which is regarded as the climatic background in lake catchment, with the reconstructed nutrient sequence of lake water and sediment are made, the hydrological variation in eutrophication process can be revealed and anthropogenic portion can also be demonstrated through linear fitting data sets, including temperature, precipitation, population, agriculture chemical fertilizer, TP of lake water, TP of sediments, etc. The characteristics of nutrient circulation during the eutrophication process can be traced by isotopic ratio ( $\delta^{13}\text{C}_{\text{org}}$ ,  $\delta^{15}\text{N}$  and  $\delta^{18}\text{O}_{\text{carb}}$ ), which reflected the isotopic composition and its bio-geochemic mechanism in different evolutionary stages.

## Simulated and reconstructed temperature in China since 1550AD

JIAN LIU<sup>1</sup>, HANS VON STORCH<sup>2</sup>, EDUARDO ZORITA<sup>2</sup>, SUMIN WANG<sup>1</sup>

<sup>1</sup> *Nanjing Institute of Geography and Limnology, Chinese Academy of Sciences, Nanjing 210008, P.R.China (jianliu@niglas.ac.cn)*

<sup>2</sup> *Institute for Coastal Research, GKSS Research Center, 21502 Geesthacht, Germany*

Research of climate change in Little Ice Age (LIA, 1550-1850AD) has received extensive concern in China. Wide-spread and severe famine and serious social turmoil have taken place in China during LIA. Also the warm conditions after the LIA had great impact on human life and national economy of China (Xu, 1998). Because of this broad interest, Climate (in particular temperature) of China since LIA has been reconstructed by Chinese scientists with a variety of proxy data, such as historical documents, tree rings, ice cores, lake sediments, archaeological materials, etc. (Yang, 2002).

Recently two long term climatic simulation experiments have been done by a consortium of scientists from Institute for Coastal Research, GKSS Research Center and other institutions. The first run, named “Christoph Columbus” (CC) was run over 535 years beginning in 1450, and is described in some detail by Zorita et al. (2003). The second run, named “Erik den Røde” (EdR), was begun in 900 and ran over 1100 years (Zorita et al., 2005). Both simulations were done with the same global atmosphere-ocean coupled climate model ECHO-G with, however, different code versions adapted to different computer systems. Reconstructed time series of the radiative effect of the presence of volcanic aerosols, greenhouse gases in the atmosphere as well as solar radiation were used as forcing. The modeling results reveal global and regional pattern of natural and anthropogenic climate change, which have some similarities with the observational record. The purpose of the present study is to compare these simulated data with observational evidence for the territory of China, and to interpret the recent changes of Chinese temperatures in the context of the forced climate model.

China can be divided into 10 districts, which are relatively homogeneous in terms of temperature, precipitation and growing season (Wang, 2001). These are northeast of China, north of China, east of China, middle of China, south of China, southeast of China, southwest of China, northwest of China, Xinjiang region and Tibet region. Based on proxies, such as temperature index, tree ring width and density,  $\delta^{18}\text{O}$  of ice core, reconstructions of temperature series have been made for all these regions via statistical techniques. The reconstructed temperature anomalies are relative to 1880-1979 (Wang, 1998).

The reconstructed decadal mean temperature anomaly series of 10 regions of China are compared to those generated in two multi-century simulations with the climate model ECHO-G, which was

forced by time-dependent volcanic aerosols, solar radiation and atmospheric greenhouse gas concentrations. The two model simulations are rather similar but exhibit some differences. Both the reconstructed and simulated developments of the temperature exhibit a “hockey-stick” pattern, with a marked increase of temperatures since the beginning of the 20th century. The variations of time scales of a few decades are, however, mostly dissimilar in the proxy-based reconstructions and in the simulations.

In general, the decadal variations are dissimilar in the reconstructed data and in the simulated data, even though the data are already heavily smoothed with a 5 decades running mean filter. The correlation between the reconstructed data and the CC-simulation for the entire period, 1590-1980, is positive (0.47 – 0.84), but these high values are essentially reflecting the presence of the hockey-stick pattern. If the two periods, pre-industrial 1590-1910 and industrial 1920-1980 are considered separately, the correlations become much smaller, namely -0.32 (region 6) to 0.72 (region 8) for the pre-industrial times, and -0.17 (region 1) to 0.32 (region 7) in modern times. Because of the heavy serial correlation in the data, the determination of significance levels is not meaningful. Interestingly, the simulated curves are among themselves rather similar, but the reconstructed series are quite different from region to region.

An attempt is made to assess whether the warming during the 20th century is within the range of “normal” variations related to solar and internal dynamical influences. It is found that the reconstructed data are well above the pre-industrial noise level of temperature fluctuations during most of the 20th century. Within the adopted framework, only the increased greenhouse gas concentrations can account for these significantly elevated temperatures. The major part of the 20th century warming can be explained only with the help of the anthropogenic greenhouse gas effect, whereas the solar effect can account only for a smaller proportion. Differently from the development in the GCM simulations, which is a steady upward trend throughout the 20th century, there is in the reconstructions a decline in the 2nd half of the 20th century. We suggest that this is reflecting the steady increase of industrial aerosol emissions in China.

#### References:

- Wang Sh-W, Gong D-Y, Zhu J-H, 2001: Twentieth century climatic warming in China in the context of the Holocene. *The Holocene*, 11(3): 313-321
- Wang Sh-W, Ye J-L, Gong D-Y, 1998: Climate of Little Ice Age in China. *Quaternary Sciences*, (1): 54-64 (in Chinese)
- Xu J-H, 1998: Sun, climate, famine and national migration. *Science in China (series D)* 41(5) 449-472 (in Chinese)



Yang B et al., 2002: Research progress on climate change during the last 2000 years. *Progress in Earth Science* 17(1): 110-117 (in Chinese)

Zorita E, González-Rouco J F, Storch H V et al., 2005: Natural and anthropogenic modes of surface temperature variations in the last thousand years. *Geophysical Research Letters*, 32, L08707, doi:10.1029/2004GL021563

Zorita E, Storch H V, González-Rouco J F, et al., 2003: Simulation of the climate of the last five centuries. GKSS Report 2003/12, 43 pp

[P-1]

## **Fission-track dating of Quaternary volcanic glass using stepwise etching**

KENTARO ITO<sup>1</sup>, NORIKO HASEBE<sup>2</sup>

<sup>1</sup> *Graduate school of Natural & Technology, Kanazawa Univ. Japan (kentaro-i@earth.s.kanazawa-u.ac.jp)*

<sup>2</sup> *Institute of Nature and Environmental Technology, Kanazawa Univ. Japan*

### Introduction

There are many wide-spread tephtras in Japan. Volcanic glass included in these tephtras shows the distinctive form, color and refractive index corresponding to type of eruption and magma chemical composition. Therefore, glass is useful for tephtra identification (Machida and Arai., 1992). For age determination of tephtra, volcanic glass has been dated by fission-track (and below FT) method (Westgate, 1989; Walter, 1989). However, FT in volcanic glass became reduced in size at ambient temperatures. The number of tracks that intersect with the observed surface, therefore the calculated FT age, was reduced. To avoid the underestimation of ages, several correction procedures were proposed (Westgate, 1989 and so on). One of the representative methods is the isothermal plateau (ITP)-FT method, which needs complicated analytical procedures, such as treatment of radioactive materials and time-consuming experiments. Here we examined a new protocol for the glass FT dating, which requires estimates of track density per unit volume using a stepwise etching experiment and measurement of <sup>238</sup>U concentration by LA-ICP-MS analysis.

### Experiment

Samples of this study are obsidian shards (JB-1, Kitada et al., 1993) from Wada Pass, Nagano Prefecture, Japan.

Samples were irradiated at the TC-Pn facility of Kyoto University Research Reactor (KUR) for two hours to obtain a known FT density per unit volume. <sup>238</sup>U concentrations were measured by the

LA-ICP-MS at Kanazawa University. Afterwards, samples were etched stepwisely to observe the increase in number of FTs through bulk etching proceeded.

## Result

An expected FT density per unit volume is calculated from the Eq. (1)

$$N_i = {}^{238}\text{N} \times I \times \sigma \times \phi \quad (1)$$

where  ${}^{238}\text{N}$  is the number of  ${}^{238}\text{U}$  per unit volume,  $I$  is the isotopic ratio of  ${}^{235}\text{U} / {}^{238}\text{U}$  ( $=1/137.88$ ),  $\sigma$  is the fission cross section ( $=5.82 \times 10^{-22} \text{ cm}^2$ ),  $\phi$  is a thermal neutron dose ( $=2.8 \times 10^{15} / \text{cm}^2 / \text{sec.}$ ).  ${}^{238}\text{N}$  is further expressed as follows (Hasebe et al., 2003).

$${}^{238}\text{N} = {}^{238}\text{U} \times 10^{-6} \times (N_A / M) \times d \quad (2)$$

where  ${}^{238}\text{U}$  is a concentrations of  ${}^{238}\text{U}$  (ppm),  $N_A$  is Avogadro's number ( $=6.02 \times 10^{23}$ ),  $M$  is the mass number of  ${}^{238}\text{U}$  ( $=238$ ),  $d$  is an obsidian density ( $=2.43 \pm 0.09 \text{ g/cm}^3$ ). Measured concentrations of  ${}^{238}\text{U}$  by LA-ICP-MS analysis were 9.05-9.29 ppm. Those results indicate homogeneity of  ${}^{238}\text{U}$  in this obsidian. Resultant  $N_i$  is  $6.78 \pm 0.3 (\times 10^8 \text{ counts / cm}^3)$ .

In the stepwise etching experiment, both samples etched by 12% HF and 24% HF confirmed increase of the number of tracks with increase of etching time (Fig.1). The bulk etching rate ( $V_g$ ), which is necessary to know the volume from which the observed FTs were recovered, were estimated with two ways (a) Actual measurement of obsidian thickness before and after etching by micrometer (b) Estimate based on the increase in track radius. The image processing soft "ImageJ" was used for measurement of track radius.

$V_g$  estimated from radius increase and  $V_g$  from micrometer correspond well within analytical errors (Fig.2). Furthermore, the induced track density estimated thorough stepwise etching corresponds well to the known value from Eq. (1) (Fig.3).

## Reference

- Hasebe, N., Barbarand, J., Carter, A. and Hurford, T. (2003), Fission Track News Letter, 16, 1-5.
- Kitada, N., Wadatumi, K. and Masumoto, S. (1993), Fission Track News Letter, 6, 11-12.
- Machida, H. and Arai, F. (1992), Atlas of Tephra in and around Japan.
- Walter, R. C. (1989), Quaternary International, Volume 1, 35-46.
- Westgate, J. A. (1989), Earth and Planetary Science Letters, 95, 226-234.

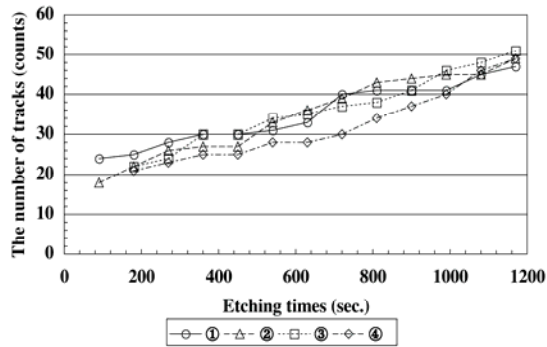


Fig.1 The accumulated number of tracks against etching duration. (Ex. 12% HF).

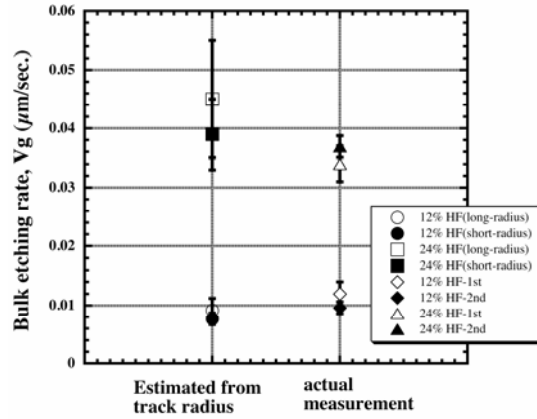


Fig.2 The comparison of  $V_g$  estimated from the track radius and

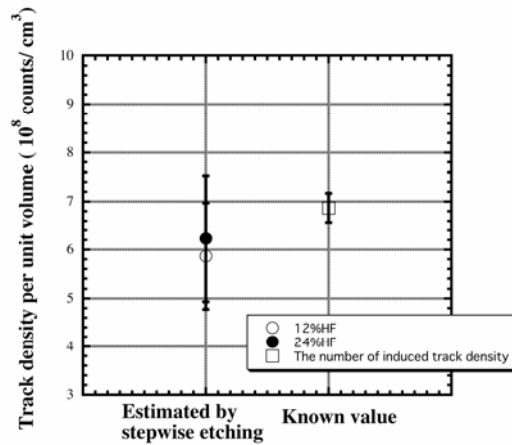


Fig.3 The comparison of FT density between the known value and the estimated value from stepwise etching.

[P-2]

## Continental margin development: Fission track data from accretionary complexes, southwest Japan

NORIKO HASEBE<sup>1</sup>, KOMEI ARATA<sup>2</sup>

<sup>1</sup>Institute of Nature and Environmental Technology, Kanazawa University, Japan  
(hasebe@kenroku.kanazawa-u.ac.jp)

<sup>2</sup>Department of Earth Sciences, Kanazawa University, Japan

The Japanese Islands consist mainly of late Palaeozoic to Cenozoic accretionary complexes that formed along a subduction zone at the East Asian continental margin. Understanding of the evolution of accretionary complexes is important because of its critical role in a horizontal growth of continental crusts and potential as a recorder of the past events occurred in subduction zones. This study compiles fission track thermochronological data from southwest Japan to investigate the evolutionary history of the area. The data are from Kyushu, Shikoku, Kii, Gifu and Shizuoka from west to east.

The data shows that, except for samples which underwent local heating by the intrusive bodies, northern samples accreted earlier reached the higher maximum temperature during accretionary processes in the outer zone of Japan. This is explained by the accretionary processes of two stages; buried stage and exhumation stage. Northern samples have stayed in the exhumation stage relatively long resulting in the exposure of samples with deeper maximum burial. Samples from the Inner Jurassic accretionary complex (Mino Belt, Gifu region) yield older fission track zircon ages than that from the Sambagawa and Shimanto belts. Cooling ages through the apatite closure temperature are older in north than in south. This explains that exhumation would not last forever and stopped at some point. The exhumation would be caused by the events such as rapid subduction of the Shikoku Basin, or would be explained by the general underplating mechanism which supply material at the bottom of accretionary wedge and force the deformation and uplift of the prism. Especially in the Shizuoka area, uplift and erosion process has been very active resulting in very young Quaternary cooling ages of the area, caused by the collision of the Izu-Bonin arc against Japanese main Islands. Erosion processes also must play an important role to remove the surface material. However little is known about the relationship between present-day erosion rate and cooling age distribution.

[P-3]

## **Local and global environmental fluctuations inferred from terrestrial sediment information**

MASANARI INUKAI<sup>1</sup>, KENJI KASHIWAYA<sup>2</sup>

<sup>1</sup>*Graduate School of Natural Science and Technology, Kanazawa University, Japan  
(masanari@earth.s.kanazawa-u.ac.jp)*

<sup>2</sup>*Institute of Nature and Environmental Technology, Kanazawa University, Japan*

This study mainly aims to clarify sedimentation processes and sediment information in a small pond called Takidani-ike, Kanazawa, Japan, additionally eolian dust sediments in surrounding areas are also studied. The mean annual precipitation is about 2400mm and snowfall days are about 53 days in Kanazawa during the last ten years. Takidani-ike is used for agricultural purpose, thus water level often fluctuate in farming season (Mar-Sep). We have set sediment traps on the bottom surface of pond since June, 2000. Sediments in the traps are taken up nearly once for a month. Eolian dust sediment traps have been set at Takidani-ike and the Kakuma tower in Kanazawa university campus (Takidani-ike since March 2003, the tower since April 2005). Eolian dust sediments are taken up once or twice for a month.

Analytical results for the Takidani-ike pond-catchments system show that

- 1) seasonal sedimentation rate is proportional to seasonal rain fall except winter season,
- 2) monthly sedimentation rate is inversely related to monthly precipitation (snow) in winter season,
- 3) monthly sedimentation rate in summer and autumn is closely related to change in water level; sedimentation rate seems to increase at times after long low water level.

Analytical results for eolian sediment information indicate that

- 1) sedimentation rate (in eolian dust traps) increase in Kosa season (Feb-Mar),
- 2) increase in grain size (4-11 $\mu$ m) content is correspond to increase in Kosa.

[P-4]

## Luminescence characteristics of lake sediments in Baikal

KAZUMI ITO<sup>1</sup>, NORIKO HASEBE<sup>2</sup>, YOSHIHIRO GANZAWA<sup>3</sup>, KENJI KASHIWAYA<sup>4</sup>

<sup>1</sup> Graduate School of Natural Science and Technology, Kanazawa Univ. ([kazumi-i@earth.s.kanazawa-u.ac.jp](mailto:kazumi-i@earth.s.kanazawa-u.ac.jp))

<sup>2</sup> Institute of Nature and Environmental Technology, Kanazawa University, Japan

<sup>3</sup> Institute of Earth Science, Hokkaido University of Education, Japan

<sup>4</sup> Institute of Nature and Environmental Technology, Kanazawa University, japan

### 1. Introduction

Lake sediments yield continental records of past environmental fluctuation and dating is important to extract quantitative information from those sediments. Luminescence dating is applicable to middle to late Quaternary samples, and basically applied to a particular mineral such as quartz, feldspar and so on. However, fine grained samples with limited quantities are difficult to apply mineral separation. Therefore, this study examines luminescence characteristics of polymineral lake sediments.

### 2. Purpose of this study

The best experimental condition is sought for infrared stimulated luminescence (IRSL), red and blue thermoluminescence (RTL and BTL) methods. The relationship between given dose and luminescence intensity is examined to see the effect of grain size variation and organic matter incorporation. To understand what resets luminescence ages, samples are exposed to artificial lights to see a decrease of luminescence signal. Also, to investigate the measurable age range, a saturated dose is estimated. Finally, equivalent dose ( $D_e$ ) is measured for particular lake sediments.

### **3. Sites and Samples**

Sediment samples were collected from the deepest part of Central Basin (M-14) and Academician Ridge (VER98 st.5) of Lake Baikal. Detailed descriptions can be found in Sasaki (2002MS) and Nakagawa (2000MS). An analyzed sample (4A-18) from VER98 was obtained at a depth of 700 cm from the lake bottom and expected age based on oxygen isotope ratio stage is 200 ka.

### **4. Experimental method**

The M-14 was divided into four aliquots according to grain sizes (in microns), that is, 6-11, 11-17, 17-32, 75-125. An aliquot without grain size separation called “all” was also analyzed. A part of aliquots 11-17 and “all” was further treated using  $H_2O_2$  to remove organic matter. No treatment was applied to the 4A-18. The IRSL, RTL and BTL were measured at Hokkaido University of Education. The M-14 was used for a dose recovery test (Tsukamoto, 2005), a breach test and a measurable age range test and 4A-18 was used for  $D_e$  measurement.

### **5. Result and conclusion**

#### **M-14**

The RTL is mainly emitted at 150°C and 250°C. A peak at 150°C is attributed to the unstable luminescence against heat. Signals, calculated by integration of luminescence intensities at the temperature range of 240~260°C, show an excellent stable linear relationship against given doses. However, artificial accumulated dose was overestimated and an excess dose is about 25Gy at an average. Effects of grain size and organic matter on luminescence are negligible. Sensitivity change through the repeated sequence for IRSL is not systematic, and linear relationships between the given dose and luminescence signal are not clear. Therefore, measurement condition of IRSL is not yet determined for this sample.

Breach tests show that an intensity of RTL reduces down to 30% and that of IRSL reduces down to 5% by the exposure to the sun light.

To investigate the age limit applicable by the RTL and BTL methods, doses up to 960Gy were irradiated. Calibration curves are bent at ~700Gy for RTL and at ~500Gy for BTL, but are not saturated up to 960Gy. IRSL data precision was not good enough to obtain calibration curves.

$D_e$  was calculated by the RTL measurement after residual dose were estimated. Residual dose was about 36Gy of apparent  $D_e$ . Average  $D_e$  of 9 aliquots was 143Gy. Calibration curve of IRSL was so good that  $D_e$  was also calculated to be 189Gy by the IRSL measurement.

## 6. Summary

RTL and IRSL are mainly measured for this study using two samples. Effects of grain size and organic matter on luminescence are negligible, therefore no sample treatment for the 4A-18 was appropriate. Overestimated of artificial accumulated dose for the 4A-18 is caused by the residual dose. The sensitivity change of IRSL through the repeated sequence is not systematic for the M-14, but is systematic for the 4A-18. The estimated  $D_e$  for the 4A-18 shows discrepancy between values obtained by IRSL and RTL.

## 7. References

- Sasaki Miki (2002MS): Recent Limno-geomorphological Environment in Baikal Region Inferred from Surficial Lake Sediments and Its Surrounding Environmental Information
- Hirofumi Nakagawa (2000MS): Climato-limnological signals found in physical properties and biogenic silica content of bottom sediments from Lake Baikal during the past several hundred thousand years
- Tsukamoto (2005); Recent development in luminescence dating; on the extending the age range and the behavior of different OSL components from quartz, *Jour. Geol. Soc. Japan*, Vol. 111, No. 11, p. 643-653

[P-5]

## **Hydro-environmental fluctuations around Lake Biwa during the past several hundreds years inferred from lake sediment information**

TAEKO ITONO<sup>1</sup>, KENJI KASHIWAYA<sup>2</sup>

<sup>1</sup>*Graduate School of Natural Science and Technology, Kanazawa University, Kanazawa, Ishikawa 920-1192 Japan (itono@earth.s.kanazawa-u.ac.jp)*

<sup>2</sup>*Institute of Nature and Environmental Technology, Kanazawa University, Kanazawa, Ishikawa 920-1192 Japan*

Lake sediments have high resolution sequential records on its surrounding catchments and global environmental fluctuations such as climate fluctuation. Therefore lake sediments are suitable to reconstruct past hydro-environmental fluctuations.

Lake sediment cores were obtained in the Shiozu Bay on the northern part of Lake Biwa and near the Ado River on the central part of Lake Biwa. Here we discuss in order to infer hydro-environmental fluctuations around Lake Biwa on the basis of physical properties of lake sediment information.

Isewan Typhoon is recorded in the Short core. There is a good relationship between 100mm excess daily rainfall and mineral grain size during the past 45 years from surface core samples indicating that mineral grain size may be available for “rain gauge” (Fig.1).

The fluctuation in mineral grain size also seems to suggest that Medieval Warm Period and Little Ice Age are recorded in the sediment.

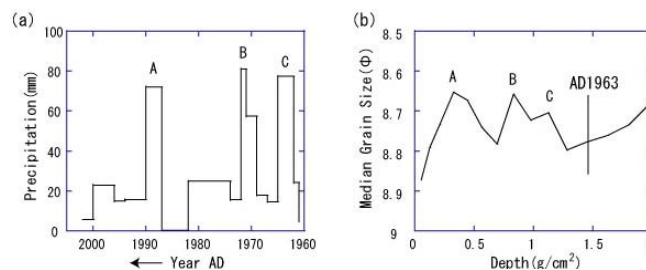


Fig.1. (a) 100mm excess daily rainfall in Hikone, the east of Lake Biwa. (b) Mineral grain size from surface core sample.

[P-6]

## Geochemical review of the Upo Holocene sediments, southern part of Korea

HYUN-SOO YUN<sup>1</sup>, WOOK-HYUN NAHM<sup>1</sup>, SEI-SUN HONG<sup>1</sup>

<sup>1</sup>*Korea Institute of Geoscience and Mineral Resources, Korea (hyuns@kigam.re.kr)*

### 1. Introduction

The Upo wetland is the largest and natural riverline wetland in the Changnyeong, southern part of Korea. It developed along the lower Topyeong tributary, eastern part of the Nakdong River. Along the Topyeong tributary, there is a knickpoint boundary between sedimentary and volcanic rocks. Based on the boundary, they are low and high altitudes in topography, and western flat and steeply eastern mountainous parts, respectively. To know the minerals of the Upo wetland sediments, representative samples were taken from the UP-1 core and bottom, respectively, and were analyzed by XRD. And the core samples were also analyzed to interpret the geochemical characteristics of major, and trace and rare earth elements, respectively.

### 2. Stratigraphy and minerals



In stratigraphy, UP-1 core is divided into four units (Nahm et al., 2006). From the ascending order, Unit 1 sediments generally consist of clayey silt. Unit 2 mainly consists of very fine silt and clay with no vertical textural changes. Unit 3 contains abundant silt and sand grains, and at the lower part of the unit, three sand layers are developed in the clayey silt. Unit 4 represents mottled clayey silt of soft to firm.

From the XRD analysis results, the core sediments consist of quartz, plagioclase, k-feldspar, hornblende, chlorite, kaolinite, illite and so on. Among them, hornblende is partly developed in very small amounts through the whole units. The others of the major compositions are wholly included all over the units. Illite shows relatively smaller in amounts than kaolinite. And plagioclase generally shows more abundant in amounts than k-feldspar. Bottom sediments of the Upo wetland show almost the same mineral compositions as the core.

### 3. Geochemical characteristics

#### 3-1. Major element

In stratigraphy, UP-1 core is divided into four units (Nahm et al., 2006). Unit 1 were deposited probably due to the repeated sedimentation cycles of accumulation, denudation and soil-forming processes, which might cause the undulations of  $\text{Al}_2\text{O}_3$ ,  $\text{Fe}_2\text{O}_3(\text{t})$ ,  $\text{MgO}$ ,  $\text{CaO}$ ,  $\text{Na}_2\text{O}$ ,  $\text{SiO}_2$  and LOI compositions. Unit 2 and 3 show no laminar or cross-bedding structures, which could indicate stable wetland environments of relatively homogeneous sediments. From the whole variations of major elements, relatively homogeneous sediments might be generally accumulated during the deposition of the Upo wetland.

At the deposition time of the sand layers, lower part of the Unit 3, there might be occurred slightly strong events of environmental change around the Upo wetland. Quartz and feldspars, which are predominated in  $\text{SiO}_2$ ,  $\text{K}_2\text{O}$  and  $\text{Na}_2\text{O}$ , were more flowed in than those of the other units. And it may be also postulated that clay components predominant in  $\text{Al}_2\text{O}_3$  were more flowed out downstream, and LOI contents were decreased thereby.

#### 3-2. Trace and rare earth elements

Besides Zn and Ba, V, Cr, Co, As, Sc, Cs, Rb, Sb, Ta and Hf mostly show no special trends, and have very narrow content ranges of variations. At the lower part of the Unit 3, V, Cr, Zn and Ba have more or less decreasing in contents, and Rb somewhat increasing ones. Their whole trends and narrow contents can suggest that the Upo sediments were deposited relatively homogeneous. And at the lower part of the Unit 3, the events of environmental change might cause the differences of somewhat dominant sediments such as quartz, feldspars and potassium minerals.

Chondrite-normalized REE of the Upo sediments are also fallen in the fields of NASC (North American shale composite), PAAS (Post-Archean average Austrian shale) and ES (European shales), and the modern river sediments. And they have also similar patterns as those (Taylor and McLennan, 1985) of NASC, PAAS, ES and the modern river sediments. During the deposition

times of the lower part of Unit 3, sandy grains, such as dominant quartz and less feldspars, were supplied into the Upo wetland by surface environment changes.

#### 4. Conclusions and discussions

The core sediments in XRD and geochemical analysis reveal that relatively homogeneous sediments were generally accumulated during the deposition of the Upo wetland. Unit 1 was deposited due to the repeated sedimentation cycles, which might cause the undulations of  $\text{Al}_2\text{O}_3$ ,  $\text{Fe}_2\text{O}_3$  (t),  $\text{MgO}$ ,  $\text{CaO}$ ,  $\text{Na}_2\text{O}$ ,  $\text{SiO}_2$  and LOI compositions. And at the lower part of Unit 3, quartz and feldspars which are more abundant in  $\text{SiO}_2$ ,  $\text{K}_2\text{O}$  and  $\text{Na}_2\text{O}$  compositions were more flowed in than the other unit parts. And clay components predominant in  $\text{Al}_2\text{O}_3$  compositions were more flowed out downstream. These can be also a main factor of decreasing CIA (Nesbitt and Young, 1982) at the lower part. Ba and Rb of a weakly positive relation have 700 ppm and 110 ppm, and 425 ppm and 90 ppm, respectively. Their contents show very close contents to the crustal average rather than upper continental crust (UCC) (Gromet et al., 1984; Taylor, 1964). Chondrite-normalized REE can represent that the source rocks of the Upo sediments were representative of the UCC materials. And the remarkably uniform patterns can also reveal that the UP-1 was deposited of sediment materials from almost homogeneous sources.

In the sand layers in Unit 3, temporary elimination of woodland covering by forest fire can be considered a possibility of the soil erosions. In such circumstances, a little charcoals are generally deposited in the sediments (MacDonald *et al.*, 1991; Odgaard, 1992; Pitkanen and Huttunen, 1999). In the sand layers, any charcoal layers can't be observed. Charcoals and sediments of relatively low and high specific gravity, respectively, can also be separated by various sedimentary mechanisms (Patterson et al., 1987). It seems the most reasonable to judge that the sand layers were related to rainfall, its related flood and so on. Concentrated rainfalls would also be able to transport the soil part eroded to the Upo wetland region. In the sand layers, special sedimentary texture and fining upward aspects can't be seen.

#### References

- Gromet, L.P., Dymek, R.F., Haskin, L.A., Koretev, R.L., 1984. The "North American shale composite": its compilation, major and trace element characteristics. *Geochim. Cosmochim. Acta* 48, 2469-2482.
- MacDonald, G.M., Larsen, C.P.S., Szeicz, J.M., Moser, K.A., 1991. The reconstruction of Boreal forest fire history from lake sediments: a comparison of charcoal, pollen, sedimentological and geochemical indices. *Quaternary Science Reviews* 10, 53-71.
- Nahm, W.H., Kim, J.K., Yang, D.Y., Kim, J.Y., Yi, S., Yu, K.M., 2006. Holocene paleosols of the Upo wetland, Korea: their implications for wetland formation. *Quaternary International* 144, 53-60.

- Nesbitt, H.W., Young, G.M., 1982. Early Proterozoic climates and plate motions inferred from major element chemistry of lutites. *Nature* 299, 715-717.
- Odgaard, B.V., 1992. The fire history of Danish heathland areas as reflected by pollen and charred particles from lake sediments. *Holocene* 2, 218-226.
- Patterson, W.A., Edwards, K.J., MacGuire, D.J., 1987. Microscopic charcoal as a fossil indicator of fire. *Quaternary Science Reviews* 6, 3-23.
- Pitkanen, A., Huttunen, P., 1999. A 1300 year forest-fire history at a site in eastern Finland based on Charcoal and pollen records in laminated lake sediment. *Holocene* 9, 311-399.
- Taylor, S.R., McLennan, S.M., 1985. *The continental crust: its composition and evolution*. Blackwell Scientific Publications, Oxford London Edinburgh Boston Palo Alto Melbourne, 312 pp.

[P-7]

## **Geochemistry of riverbed sediments of the Seomjin River in the Sunchang area, Korea**

SEI-SUN HONG<sup>1</sup>, JAE-HO KWAK<sup>1</sup>, DONG-YOON YANG<sup>1</sup>

<sup>1</sup>*Korea Institute of Geoscience and Mineral Resources, Korea (hss@kigam.re.kr)*

Riverbed sediments are produced by weathering of bedrocks, transportation and deposition. They are very important to verify the source materials for provenance and to know the process of the sedimentary movement. This study was carried out in order to understand how riverbed sediments in the Seomjin River were related to the adjacent source rock around the Sunchang area. The branch rivers studied are Kyong-cheon and Okgwa-cheon streams which pass through Sunchang-eup and Okgwa-eup, respectively, and Seobong-cheon stream at Seobong-ri, Gogseong-gun, and the main Seomjin river.

The studied area is composed of the Granitic gneiss, Seologri Formation, Mesozoic granite, and Cretaceous volcanics. About 1 kg of sediments from the dig hole with depth of 30cm were taken in the drainage area. These samples should be dried before sieving to obtain 100~200g of -100 mesh sediments.

SiO<sub>2</sub> composition show comparatively wide range from 55 wt.% to 78wt.%. In general, as the amount of SiO<sub>2</sub> increases, that of TiO<sub>2</sub>, Al<sub>2</sub>O<sub>3</sub>, Fe<sub>2</sub>O<sub>3</sub>(t), MnO, MgO, CaO, P<sub>2</sub>O<sub>5</sub> decreases, while K<sub>2</sub>O show increasing trend and Na<sub>2</sub>O pattern is slightly decreasing. The content of TiO<sub>2</sub>, Fe<sub>2</sub>O<sub>3</sub>(t), MnO, MgO, CaO in sediments are higher than those of bedrock samples. But Na<sub>2</sub>O, K<sub>2</sub>O, Al<sub>2</sub>O<sub>3</sub> contents is lower than those of bedrock.

The differences in the chemical composition are more obvious in four streams.  $\text{TiO}_2$ ,  $\text{Fe}_2\text{O}_3$  (t),  $\text{CaO}$  contents of sediments from Okgwa stream tend to be lowest for given  $\text{SiO}_2$ , compared with those of other streams. In Kyong-cheon, composed of foliated granites,  $\text{TiO}_2$ ,  $\text{MgO}$ ,  $\text{CaO}$ ,  $\text{K}_2\text{O}$ ,  $\text{Na}_2\text{O}$  contents show no variations from upstream to downstream, but  $\text{Al}_2\text{O}_3$ ,  $\text{Fe}_2\text{O}_3$ (t),  $\text{P}_2\text{O}_5$  contents are slightly increasing. In Okgwa-cheon, composed of meta-sedimentary rocks and granites, similar trends can be found for  $\text{TiO}_2$ ,  $\text{MgO}$ ,  $\text{CaO}$ ,  $\text{Na}_2\text{O}$ . Especially in the Seobong-cheon that are distributed by meta-sedimentary rocks, the contents of transition elements such as  $\text{TiO}_2$ ,  $\text{Fe}_2\text{O}_3$  (t),  $\text{MgO}$ ,  $\text{P}_2\text{O}_5$ , are highest value of all streams.

From the geochemical data, major element variations show a rather gradational than with a sharp variation from upstream to downstream and can reflect the bedrock geology.

[P-8]

### **The fluctuation in trace element concentrations from the Cheollipo coast, Korea**

DONG-YOON YANG<sup>1</sup>, JU-YONG KIM<sup>1</sup>, WOOK-HYUN NAHM<sup>1</sup>, SANGHEON YI<sup>1</sup>, JIN-YOUNG LEE<sup>1</sup>,  
JIN-KWAN KIM<sup>1</sup>

<sup>1</sup>*Korea Institute of Geoscience and Mineral Resources, Korea (ydy@kigam.re.kr)*

The analyses of trace elements from CL4 borehole core drilled in the Cheollipo wetland were carried out to verify eolian input and the formation of evaporites of Korean western coast during the Holocene time.

Based on the geochemical proxies ( $\text{Na}/\text{Al}$ ,  $\text{Si}/\text{Al}$ ,  $\text{Zr}/\text{Al}$ ,  $\text{Sr}/\text{Ba}$  and  $\text{Ca}/\text{Mg}$ ) and evaporite mineralogy, the depth profile is divided into two geochemical zones of variable sediment-water interaction, evaporation and eolian activity. The upper zone during the late Holocene enriched in gypsum but poor in traces is characterized by lower chemical weathering during 2500-2000 yr BP, higher eolian activity about 2100 yr BP and evaporation especially during 4500-4300 yr BP and during 2400-1700 yr BP. The lower zone during the early Holocene is enriched in traces and reflects higher chemical weathering in the catchments. Especially, the high contents of As and U between 7400 yr BP and 4500 yr BP indicate that that the wetland was affected directly and/or indirectly by sea-water, because seawater is the dominating source for As and U.

The remaining trace elements seem to have a freshwater source. However the high concentration in Cu and Zn contents is shown in CL 4 core of Cheollipo around 2100 yr BP. The groundwater and the seawater in the investigated area are characterized by the high values of 151-199  $\mu\text{g}/\text{l}$  and 28.5-109  $\mu\text{g}/\text{l}$  in Zn and Cu contents, respectively. But the high content of Cu in sea water is presumed

being limited only in the investigated area, because the average contents of Cu in the Korean West-sea is very low (0.42-1.23  $\mu\text{g/l}$ ). Consequently, these phenomena may indicate the high content in lithogenic Cu and the human intervention such as mining activity of Bronze ages in the area.

Further studies can solve the problem why can the high content of seawater in Cu be preserved in the investigated coast now.

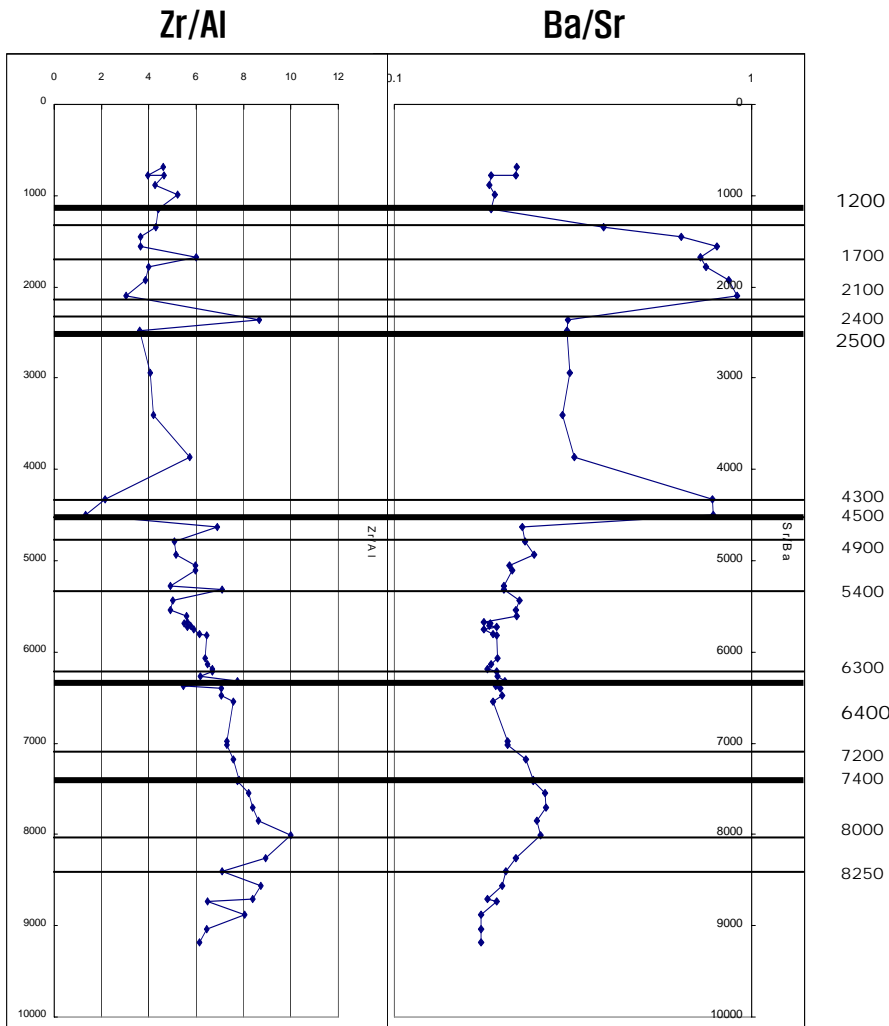


Fig. 1. The ratios of Zr/Al and Ba/Sr indicate the degrees of eolian input and evaporation respectively.

[P-9]

**Variations in organic matter composition in a maar sediments from Cheju Island, Korea, during the last 6500 years: implications for environmental changes**

JAESOO LIM<sup>1</sup>, EIJI MATSUMOTO<sup>1</sup>

<sup>1</sup>Graduate School of Environmental Studies, Nagoya University, Japan (s020121d@mbox.nagoya-u.ac.jp)

In order to track changes in the relative abundance of C<sub>3</sub> and C<sub>4</sub> plants, total organic carbon content (TOC), total nitrogen content (TN), and organic carbon isotopes ( $\delta^{13}\text{C}$ ) were measured on bulk organic matter in a maar sediments of Cheju Island, Korea. High C/N ratios ranging from 14 to 26 during the last 6500 years suggest that terrestrial plants (C<sub>3</sub> and C<sub>4</sub> plants) mainly formed the organic matter in the maar. The  $\delta^{13}\text{C}$  values of the organic matter varied between  $-29\text{‰}$  and  $-18\text{‰}$ , revealing a long-term decreasing trend during the last 6500 years. The long-term decreasing trend of  $\delta^{13}\text{C}$  values suggests decrease in C<sub>4</sub> plants and increase in C<sub>3</sub> plants in the study areas. This is confirmed by pollen records showing gradual increase in arboreal pollen during the last 6500 years. The large-scale variation of C<sub>3</sub> and C<sub>4</sub> plants in Cheju Island during the last 6500 years may be affected by changes in the solar insolation and the strength of the East Asian summer monsoon. The C/N ratio,  $\delta^{13}\text{C}$  values of bulk organic material, and pollen data from other maars and lakes in East Asia may be useful as indicators of terrestrial vegetation changes and provide chances to understand environmental changes in the past.

[P-10]

## **Long Range Transport of PAHs with Asian Dusts from Eastern Asian Continent to Japan -Stability of PAHs on Mineral Surfaces-**

SHUJI TAMAMURA<sup>1</sup>, TSUTOMU SATO<sup>1</sup>, YUKIE OTA<sup>1</sup>, NING TANG<sup>2</sup>, KAZUICHI HAYAKAWA<sup>2</sup>,  
TETURO YONEDA<sup>1</sup>

<sup>1</sup>Graduate School of Hokkaido University, Japan

<sup>2</sup>Graduate School of Kanazawa University, Japan

Polycyclic aromatic hydrocarbons (PAHs) are organic compounds originated by incomplete combustion of fossil fuel and released in the atmosphere in gas and aerosol phase. Because of their toxicity, environmental behavior of PAHs has attracted much attention. Long-range transport of PAHs has been known in various locations in the world for a long time already. However, such an issue has not been investigated from eastern Asian continent over Japan Sea even growing emissions are expected there by rapid industrial development. Anthropogenic sulfate and nitrate can accumulate on Asian dust particles during its transport in the atmosphere. Although there is a great probability that PAHs would adsorbed on dust particles, there is very little understanding on its

nature and fate. In this study, aerosol particles have been collected from April 2003 for a year in the rural areas of Kanazawa, Ishikawa, JAPAN with the main objective of understanding the role of Asian dust in the atmospheric circulation of PAHs over long distances. Three sampling intervals have been designated in this study, namely: (1) Dust Period 1 (March 11 to 19, 2003); (2) Dust period 2 (March 28 to April 9, 2003); and (3) Dust period 3 (April 9 to 25, 2004). The Asian dust particles are dominantly in the coarse particle size range (2.1-11 $\mu$ m). The analyses for PAHs were performed separately in both coarse and fine particle range (<1.1 $\mu$ m). Seasonal trend of PAHs concentrations in coarse and fine particles showed Asian dust particles in Dust period 3 contained significant amount of less volatile PAHs such as Benzo[a]pyrene (BaP) and Benzo[g,h,i]perylene (BghiP). A kinetic model developed in this study revealed that these PAHs would be hardly accumulated on Asian dust particles in the atmosphere due to their extremely slow sorption rate. These PAHs would have to be originally PAHs-polluted soil particles. Back trajectory analyses would suggest that the Asian dust in Dust period 3 would have come from around the industrialized areas of the loess plateau. The stabilities of PAHs on mineral particles under controlled temperature and relative humidity (RH) with and without light irradiation were investigated. The aim was to understand the stability of PAHs associated with different components of Asian dust particles during transport over long distance. Pyrene (Pyr) was chosen as a model PAHs. Quartz showed a strong catalytic effect (i.e. enhances) in the decomposition of Pyr even with a coating of sorbed humic acid and without light irradiation (i.e. placed in the dark). Pyr sorbed on montmorillonite remained stable in the dark throughout the experimental period (3 day). Moisture in the experimental cell also decreased the stability of Pyr especially on  $\alpha$ -alumina. Light irradiation decreased the stabilities of Pyr on quartz and montmorillonite, while the decomposition rate on montmorillonite was slower than on quartz in the dark. Photochemical degradation of Pyr on humic acid was not observed. PAHs sorbed on quartz and feldspar in Asian dust would be decomposed rapidly due to the catalytic role of silanol and aluminol sites on the mineral surface. The catalytic effect are enhanced further by light irradiation and elevated RH during transport over the Sea of Japan. Although a high RH and light irradiation could reduce PAHs stability on clay minerals, a considerable amount would still remain to last for several days. Humic acid in Asian dust particles would protect PAHs most efficiently from decomposition against high RH and light irradiation, but their influence would be minor due to their small amount in the Asian dust particles. The most realistic carrier of PAHs in the Asian dust over long distance would be clay minerals instead of humic acid. Geologic materials would play significant role for atmospheric circulation of PAHs than previously thought

## Holocene depositional processes recorded in the borehole data sets around the lower reach of Han River, the middle part of the Korean Peninsula

JIN YOUNG LEE<sup>1</sup>, DONG YOON YANG<sup>1</sup>, JU YONG KIM<sup>1</sup>, SEI SUN HONG<sup>1</sup>

<sup>1</sup>*Korea Institute of Geoscience & Mineral Resources, Korea,*

The sediment sequences recovered from 125 drilling holes in the Hanam Pungsan land development area are investigated to understand the late Pleistocene and Holocene environmental changes around the lower reach of Han River. Twenty five cross-sectional profiles drawn from the borehole stratigraphic descriptions indicate that the several stages of fluvial geomorphological development occurred during the late Pleistocene and Holocene. Several fluvial depositional settings including channel, natural levee and back swamp can be distinguished by the profile type classification. Fluvial channel environment is typified by channel lags and sands, natural levee dominant with sands blankets, and back swamp is interbedded by peats or organic mud horizons in the typical profile types of borehole data. Further palynological and geochemical researches will be performed to ascertain the ecological and environmental fluctuation of the peat layers in the study area.

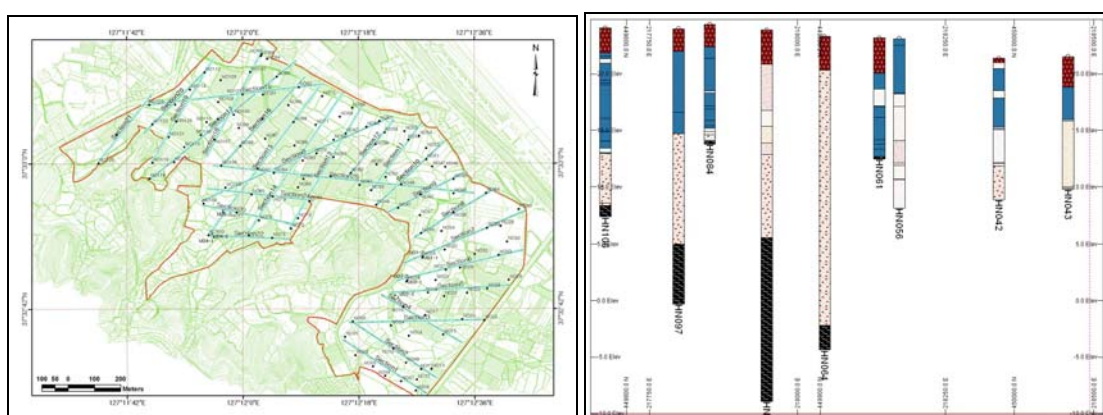


Fig. 1 Location map of drilling sites and example of section profile (No. 25).

## Holocene evolution of the Outer Lake of Hwajinpo lagoon on the eastern coast of Korea; Environmental changes with Holocene sea-level fluctuation of the East Sea (Sea of Japan)

JONG-GWON YUM<sup>1</sup>, KANG-MIN YU<sup>2</sup>, KEIJI TAKEMURA<sup>3</sup>, TOSHIRO NARUSE<sup>4</sup>, AKIHISA KITAMURA<sup>5</sup>, HIROYUKI KITAGAWA<sup>6</sup>, JONG-CHAN KIM<sup>1</sup>



<sup>1</sup>AMS Laboratory, National Center for Inter-University Facilities, Seoul National University, Seoul, 151-742, Korea. (Email: yums@snu.ac.kr.)

<sup>2</sup>Department of Earth System Sciences, College of Sciences, Yonsei University, Seoul, 120-749, Korea.

<sup>3</sup>Beppu Geothermal Research Laboratory, Institute for Geothermal Science, Graduate School of Science, Kyoto University, Beppu, 874-0903, Japan.

<sup>4</sup>Department of Geography, Hyogo University of Teacher Education, Hyogo, 673-1494, Japan.

<sup>5</sup>Institute of Geosciences, Faculty of Science, Shizuoka University, Shizuoka 422-8529, Japan.

<sup>6</sup>Institute for Hydrospheric-Atmospheric Science, Nagoya University, Nagoya 464-8601, Japan.

The evolution of the outer lake of Hwajinpo Lagoon in Korea has been reconstructed using environmental proxies (lithologic, geochemical, and fossil data) with a chronology established using 7 accelerator mass spectrometry (AMS) radiocarbon dates. Grain size, water content, and X-ray analyses from the core of outer coastal lakes (HJ99) were used to reconstruct sedimentary environments by using total organic carbon, C/N, S, and C/S chemical proxies. Assemblages of mollusc remains also provided paleoenvironmental information. The environmental changes of the outer lake of Hwajinpo Lagoon can be divided into 6 depositional phases. The basin of the Hwajinpo was exposed and underwent a weathering process before the Holocene period. The muddy sand layer on the weathered bedrock indicated an estuarine system about 6000 BP. The laminated layer implies that the lagoonal system was anoxic between about 5500–2800 BP. The marl layer implies a relatively oxic lagoonal condition with mollusc presence about 2500 BP. The layer of very low sulfur content indicates a freshwater lake system isolated by a sand barrier about 1700 BP. Beginning about 1000 BP, the river system deposits progress progradation on the marl layer. Two erosional landforms could be related with a high standing sea level span during Holocene. These high-stands are dated at 5700 BP and 2200 BP and are supposed to have formed erosional landforms of about 1.6 amsl and 0.8 amsl, respectively. Environmental changes of the outer lake of Hwajinpo Lagoon are considered due mainly to the lake- and sea-level fluctuation during Holocene.

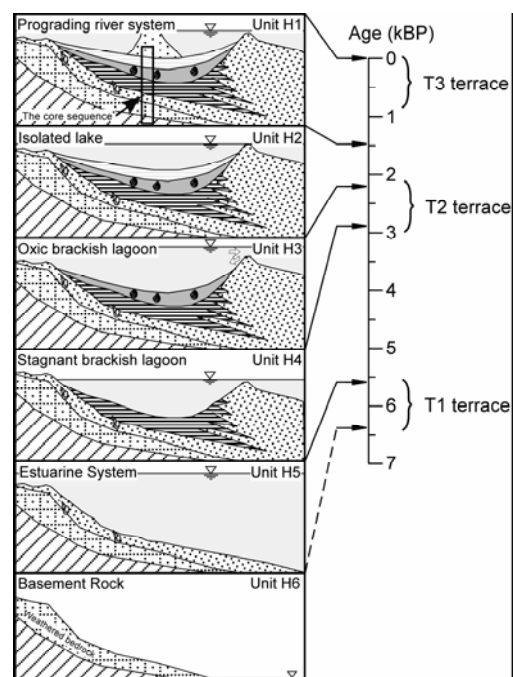


Figure 1 Conceptual evolution model of the outer lake of Hwajinpo Lagoon. The ages are estimated from <sup>14</sup>C dating on the hypothesis of a constant sedimentation rate; the sea-level changes are presented on a relative scale. Core sequence: the upper most part of the core covered with deltaic sand deposits (Unit H1); left side connected to the inner lake and right side connected to the sea side.

## Variations of Bottom Currents in the Ulleung Interplain Gap, East Sea since the Last Glacial Maximum: Evidences from Grain Size Analysis

JANG-JUN BAHK<sup>1</sup>, JAE-HWA JIN<sup>1</sup>

<sup>1</sup>*Korea Institute of Geoscience and Mineral Resources, Korea (jjbahk@kigam.re.kr)*

The Ulleung Interplain Gap (UIG) is a deep narrow (ca. 2500 m deep and 75 km wide) passage which has served as a conduit for deep-water circulation between the Ulleung and Japan basins of the East Sea (Sea of Japan). The late Quaternary sedimentation in the deep passage was known to be dominated by an interaction between bottom currents along an erosional axial channel system and downslope mass flows from its southeastern margin. In particular, relatively stronger bottom-current activity during the post-glacial period (< ~15 ka) was suggested to result in focused accumulation of resuspended sediments along the axial channel margin. In order to detail the variations of bottom currents in the UIG since the Last Glacial Maximum, we analyzed grain-size distribution of detrital fraction in a piston core sediment (05GCRP-17) from the axial channel margin of the UIG. In addition to median diameter ( $D_{50}$ ) of the whole fraction, the variability in grain-size distribution was also represented by mean diameters of sortable silt (SS: 10-63  $\mu\text{m}$ ) which is believed to be more susceptible to selective deposition and winnowing by bottom-current activity. Preliminary age controls for the core sediment were provided by 4 AMS  $^{14}\text{C}$  dates on TOC of bulk sediments and well-known tephra layers.

Lithologic unit during the post-glacial period is characterized by relatively thick (~ 4 m) muddy contourite with a few intercalated turbidite beds. The sedimentation rate during the early stage of the deglaciation (15-16 ka) is especially high (> 2 m/ka), more than 100-fold higher than the LGM. Both  $D_{50}$  and SS mean values are, in general, relatively higher during the early stage of the deglaciation and lower during the Holocene with respect to those during the LGM. In particular, the early stage of the deglaciation is punctuated by high-amplitude centennial cycles superimposed on the overall trend. Because the overall trend in  $D_{50}$  variation is generally consistent with that from a core sediment on top of the South Korea Plateau, where the bottom-current influences might have been negligible, we believe that the overall trend may reflect changes in supply of detrital sediment, rather than variations in bottom-current activity. On the other hand, the superimposed, high-amplitude centennial cycles in both  $D_{50}$  and SS mean variations during the early stage of the deglaciation, together with the extremely high sedimentation rate, suggest possible outbreak or bursting of bottom-water formation in the northern part of the East Sea in centennial scale. The bottom-current activity during that time may have been much more vigorous than the present, thus,

caused significant erosion or non-deposition in the axial channel and rapid accumulation of resuspended sediments along the channel margin.

[P-14]

## **What is the natural law that controls the responses of organisms to environmental changes?**

TAKAYOSHI KAWAI<sup>1</sup>

<sup>1</sup>*Nagoya University, Japan (tkawai@eps.nagoya-u.ac.jp)*

Since the Baikal Drilling Project started in 1989, and was followed by Baikal Hovsgol Drilling Project in 2001, this international research program has produced abundant scientific information. It seems to get more curious with various new information about the succession of organisms, “what is the natural law that controls the responses of organisms to environmental changes?” It seems not simple and easy to find the effect of climatic or environmental change on biota. To call the attention of the colleagues, several examples will be shown although the speaker is also in the dark.

- (1) Why no evolution or migration of new genera of plant occurred around Lake Baikal during a long period of 10 million years and a big climatic change from warm and wet before 5 million years to glacier-interglacial after 2.7 years ago?
- (2) Why Baikal seals moved to Lake Baikal in (or before) about 380,000 years ago, and not after this period?
- (3) Why the evolution of diatoms in Lake Baikal has been so frequent and the life time of species has been so short since glacier-interglacial period started about 2.7 million years ago?
- (4) How some diatom species survived showing their blooming with such a long interval of some million years?
- (5) How bacteria has kept alive in the sediment for millions years?
- (6) and so on.

These observations must call our new understanding about the ability and inability of life to survive the climatic and environmental changes, and our prediction concerning the effect of environmental change on biota must get more precise by clarifying above questions. Our environmental planning must be much more reliable to establish the sustainable human society surrounded by sound and thick ecosystem.

## Introduction of the Environmental Database in Pan-Japan Sea Area

TATSUTO AOKI<sup>1</sup>

<sup>1</sup>*Dept of Geography / Institute of Nature and Environmental Technology, Kanazawa University  
(kentaoki@kenroku.kanazawa-u.ac.jp)*

### Introduction

The 21<sup>st</sup> century COE program of Kanazawa University, named “Environmental Monitoring and Prediction of Long and Short-Term Dynamics of Pan-Japan Sea Area” has the following purposes,

- to enhance the international network for scientific cooperation around Japan sea area
- to collect and store the environmental datasets around Japan sea area to contribute the prediction of the environmental changes in near future

To realize these purposes, the internet-accessible database of the natural/social environmental datasets around Japan sea area is build up by our COE program. At present, however, many organizations, universities, and companies have already provides many database. So, our database tries to be the “*Portal Site (=Clearinghouse) of the Environmental Databases Pan-Japan Sea Area*”. In this presentation, the author introduces and demonstrates this database.

### Web-GIS based Database

Users of this clearinghouse would like to know the “*where* the dataset was measured (location)”, “*what* the dataset include (contents)”, and “*who* provides the dataset (provider)”. So, this clearinghouse must provide the “metadata” of each environmental database, and understand how to download / access the law data from the existing database. To realize searching “*where*”, this clearinghouse equipped web-GIS (Geographical Information System) based “Spatial (map) search” system with the map server. On this search system, users can search the location of the observation station and target area using the map (fig 1). On this system, it is possible to search not only all types of geographical encored object (point, line, and polygon), but also text based data, such as the bibliography, using “Text (keyword) search”.

### Data Format

The metadata that provided from this clearinghouse are described by the shape file format which is the native for the Arc-GIS by ESRI. This format is the *de facto* standard for the GIS. Metadata is

stored in the dbf file, but the user can not access / download this file directory through this clearinghouse.

The metadata includes following categories (see fig 3), Data ID, category, data name, simple explanation (outline), provide method, name and affiliation of data administrators, data format, data volume, period, data location (geographical coordinates), name of location, and related articles. Within these categories, first four underlined items are shown in bottom of search result window (fig 2), and other items are shown in detailed metadata window (fig 3).

### Interface of the Clearinghouse

The search window (fig 1) is subdivided into four sections. Top left is the text search window, top right is the spatial search using the coordinate, bottom left is the spatial search using map server, and bottom right is the general view window. Push “SEARCH” button, the result window (fig 2) opens. On the map section, the selected objects are indicated. Bottom of the result window, the simple metadata of the selected objects are shown. ID button of the simple metadata are related to the object on the map. Click “Detail”, the detailed metadata window (fig 3) will open as the new window. This metadata are ease to copy and paste to the database software such as MS-Excel and so on.

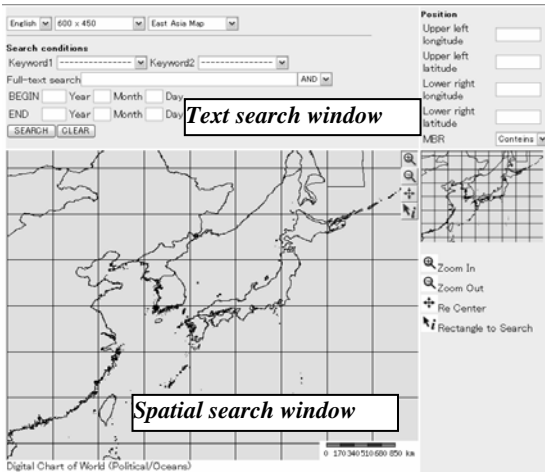


Fig 1 Search Window

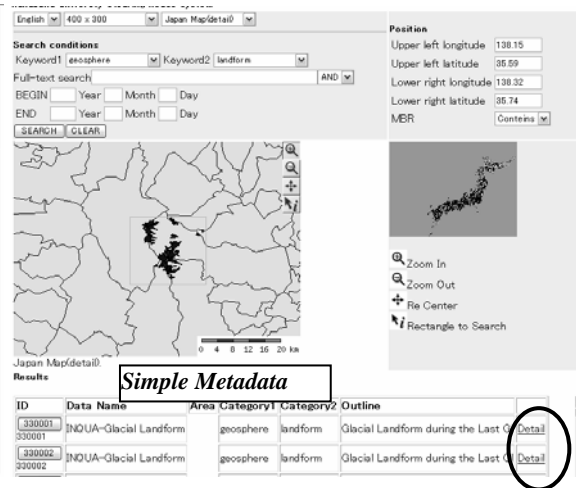


Fig 2 Search Results Window

Title	Contents
Data ID	330001
1st category	geosphere
2nd category	landform
Number of Data	1
Country of data location	Japan
Name of the dataset	INQUA-Glacial Landform
Name of the file	inqua
outline of the dataset	Glacial Landform during the Last GI
method of the data provide	3
URL of the dataset	null
policy of the data provide	please contact to the data admin
name of data administrator	Dr. Tatsuto AOKI
affiliation of the data administrator	Department of Geography, Faculty of Letters, Kanazawa Un
address of the data administrator	Kakuma, Kanazawa, 920-1192, Ishikawa, Ja

Fig 3 Detailed metadata Window

### Call for Data

If you have the environmental data which is possible to share, please contact and send me the “metadata” of that data set. We can provide the information using our clearinghouse. Corresponding address is [kentaoki@kenroku.kanazawa-u.ac.jp](mailto:kentaoki@kenroku.kanazawa-u.ac.jp). I will send you the detailed format of the metadata.

[P-16]

## The controlling factors on mineralogy of speleothems in limestone Cave in Gangwon-do, Korea

DON WON CHOI<sup>1</sup>, KYUNG SIK WOO<sup>2</sup>, JEONG CHAN KIM<sup>1</sup>, SANGHEON YI<sup>1</sup>, DONG YOON YANG<sup>1</sup>

<sup>1</sup>*Korea Institute of Geoscience and Mineral Resources, Korea*

<sup>2</sup>*Cave Research Institute of Korea, Kangwon National University, Korea*

The speleothems, consisting of aragonite and calcite, of the Sanho Cave, Okgye Cave and Yongyeon Cave in Kangwon Province are investigated to delineate the controlling factors on mineralogy. Most speleothems show alternating layers of aragonite and calcite.

Based on stable isotopic and elemental analyses of the speleothems in Sanho, Okgye and Yongyeon Caves, the chemical changes from calcite to aragonite do not show systematic trend of Mg contents and Mg/Ca molar ratios, indicating that aragonite precipitation has little relationship with the increase in Mg/Ca ratio of the fluids. The coeval increases in the oxygen and carbon isotope contents during calcite to aragonite transition may imply that supersaturation with respect to

aragonite from rapid degassing of carbon dioxide and evaporation should have played a significant role. Also, the decrease in carbon isotope values accompanied by the decreasing Mg/Ca ratio may have resulted from the dilution effect when the supply rate of incoming fluids by seepage increased. The calculated values of Sr/Ca ratio in aragonite precipitating fluids suggest that the uptake of Sr by aragonite crystals was effective. Thus, the transition from calcite to aragonite should have been influenced by degassing of carbon dioxide and evaporation rather than the increase in Mg/Ca ratio.

Also, the presence of alternating aragonite and calcite layers may imply that mineralogy may have been controlled by microclimate variations such as humidity, temperature, partial pressure of carbon dioxide and wind.

[P-17]

## **The prediction of sediment yield change induced by landslide, South Korea – preliminary study**

MIN-SEOK KIM<sup>1</sup>, JIN-KWAN KIM<sup>1</sup>, DONG-YOON YANG<sup>1</sup>

<sup>1</sup>*Korea Institute of Geoscience and Mineral Resources, Korea (mskim@kis.kigam.re.kr)*

The information related the processes of sediment generation and transportation in catchment that causes seriously damage to life and property is a significant to manage catchments and to frame a policy. Specially, the process and quantity of the soil erosion before and after landslide occurring are different, thus, this data is very important to restore and manage place where occurred a lot of landslides. In Korea, previous reseach reported that almost landslides were transitional landslides, we applicated the SINMAP model to Yangyang-gun around Naksan temple that was developed for prediction instable slope related mainly transitional landsliding.

The input data related topography, i.e. specific catchment area and slope angle, obtained by DEM, and soil parameters, i.e. dimentionless cohesion, tan of soil internal friction angle and soil hydraulic parameter, used with default values for model and soil data around study area that the previous study reported (KIGAM, 2004), respectively. The stabiliity prediction applied with the soil data was more reliable than the prediction with default values, however, for the more detailed study, in situ soil is conducting laboratory test.

It was assumed that the instable area classfied by the SI (stability index) of SINMAP model had occurred landslide in the study area, and then this selected area input GeoWEPP model to compute the change of soil erosion and sediment yield. The results of sediment yield for before and after

landsliding using by GeoWEPP were similar with each other. However, the quantity of the soil loss per unit area after landsliding was more than three times as that of soil loss per unit area before landsliding, therefore, it will be possible to increase sediment yield on account of remained potential soil on the slope. Consequently, according to the results of soil loss and sediment yield before and after landsliding computed by the GeoWEPP model, we suggest that the trend of soil loss after landsliding increases because of vegetation removal, soil disturbance and exposed soil increasing induced by landslide.

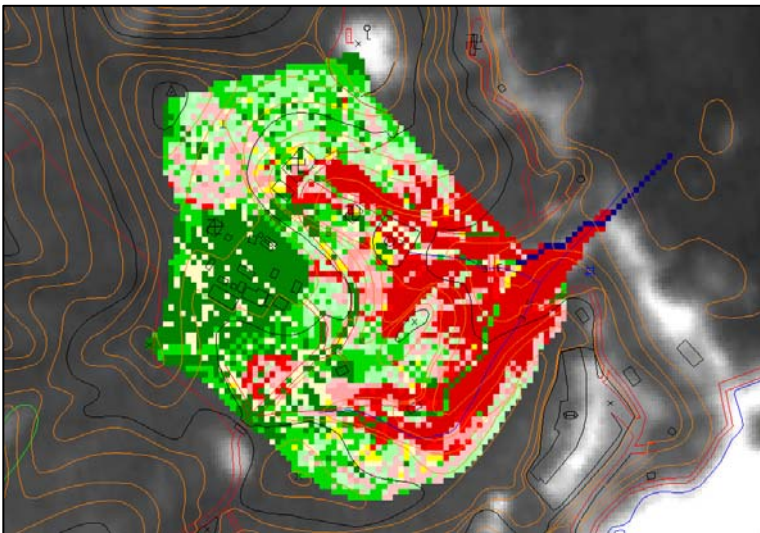


Fig.1. Soil loss map before landsliding

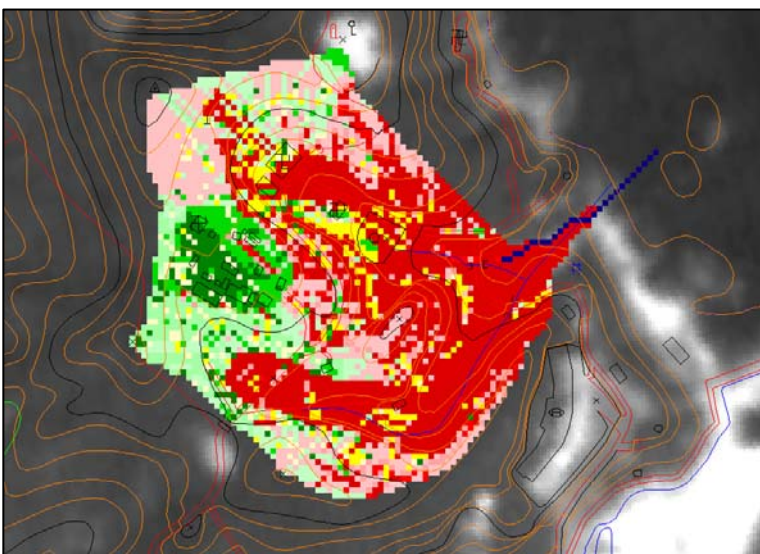


Fig.2. Soil loss map after landsliding



□ Photo

